

An adaptive perfectly matched layer finite element method for acoustic-elastic interaction in periodic structures

Sijia Li^a, Lei Lin^{a,b}, Junliang Lv^{a,*}

^a*School of Mathematics, Jilin University, Qianjin Street, Changchun, 130012, Jilin Province, China*

^b*Institute of Computational Mathematics and Scientific/Engineering Computing, Beijing, 100190, China*

Abstract

This paper considers the scattering of a time-harmonic acoustic plane wave by an elastic body with an unbounded periodic surface. The original problem can be confined to the analysis of the fields in one periodic cell. With the help of the perfectly matched layer (PML) technique, we can truncate the unbounded physical domain into a bounded computational domain. By respectively constructing the equivalent transparent boundary conditions of acoustic and elastic waves simultaneously, the well-posedness and exponential convergence of the solution to the associated truncated PML problem are established. The finite element method is applied to solve the PML problem of acoustic-elastic interaction. To address the singularity caused by the non-smooth surface of the elastic body, we establish a residual-type a posteriori error estimate and develop an adaptive PML finite element algorithm. Several numerical examples are presented to demonstrate the effectiveness of the proposed adaptive algorithm.

Keywords: acoustic-elastic interaction, perfectly matched layer, finite element method, adaptive algorithm, a posteriori error analysis

2020 MSC: 65N12, 65N15, 65N30

1. Introduction

Direct scattering [10, 23, 32, 33, 35, 40, 42] and inverse scattering [21, 26, 27, 36, 37] have long been an active area of research in applied mathematics and computational science due to their broad applications in science and engineering. In particular, the wave scattering in periodic structures [8, 45, 48], also known as diffraction gratings, plays an essential role in the design and analysis of optical components, such as increasing the efficiency of beam splitters, improving the sensitivity of optical sensors, and enhancing the performance of antireflective coatings [3, 19]. This paper is concerned with the scattering of the time-harmonic acoustic plane wave by an elastic body with an unbounded periodic surface. The region above the surface is filled with a homogeneous compressible inviscid fluid medium, while the region below is occupied by an isotropic and linearly elastic solid material. Due to the external incident acoustic field, an elastic wave is excited inside the solid, and the incident acoustic wave is scattered back into the fluid. Such a phenomenon is commonly known as the acoustic-elastic interaction in periodic structures [12, 25, 39, 47], which has received wide attention due to its significant applications in underwater acoustics and ultrasonic nondestructive evaluation [1, 18].

As in many other diffraction problems, the governing equations of acoustic-elastic interaction are formulated in unbounded domains, and the scattered and transmitted fields must satisfy appropriate radiation conditions at infinity [4]. For numerical simulation, it is essential to truncate the unbounded regions above and below the periodic interface and impose appropriate boundary conditions on artificial boundaries. For this purpose, several effective truncation methods have been proposed, such as the perfectly matched layer (PML) technique [9], the absorbing boundary conditions (ABCs) [20], and the transparent boundary conditions (TBCs) [22, 29]. In this paper, we introduce the

*Corresponding author

Email address: lvjl@jlu.edu.cn (Junliang Lv)

PML technique for domain truncation. The fundamental principle of the PML method is to design a finite-thickness absorbing layer with suitably chosen complex coordinate stretching to surround the region of interest. Due to its ease of implementation and high computational efficiency, the PML method has been widely adopted for solving various wave scattering problems, such as acoustic waves [38, 43, 44], elastic waves [11, 17, 31], electromagnetic waves [6, 7], and biharmonic waves [34]. However, due to the complexity of multiphysics coupling, a rigorous theoretical analysis of the PML method for the acoustic-elastic interaction in periodic structures is still lacking.

In practical applications, the grating profiles are often only piecewise smooth and may contain reentrant corners. Such geometric singularities usually lead to reduced regularity of the acoustic and elastic fields near the non-smooth surface, which will severely degrade the computational efficiency of uniform mesh refinement. To address this difficulty, adaptive finite element methods (AFEMs) provide an efficient numerical strategy, since they are able to concentrate computational effort only in regions where the solution exhibits singular behavior [2]. Combined with the PML technique, an efficient adaptive finite element method was firstly developed for solving the diffraction grating problem [16]. It was shown that the a posteriori error estimate consists of the finite element discretization error and the PML truncation error, where the latter decays exponentially with respect to the PML parameters, such as the thickness of the layer and the medium properties. Due to its superior numerical behavior, the adaptive finite element PML method was quickly developed to solve a variety of scattering problems, such as obstacle scattering [13, 15, 28], periodic diffraction [5, 30, 52], and open cavity problems [14]. Nevertheless, most of these results have been largely limited to single-physics scattering problems. For the problem of acoustic-elastic interaction in periodic structures, the rigorous a posteriori analysis remains underdeveloped.

Motivated by these considerations, the current paper develops and analyzes an adaptive perfectly matched layer finite element method for the acoustic-elastic interaction in periodic structures. We firstly derive a truncated PML formulation of acoustic-elastic interaction and establish its well-posedness. Moreover, we provide a rigorous convergence analysis showing that the PML approximation error decays exponentially with respect to the acoustic and elastic PML parameters simultaneously. Based on the truncated PML formulation, we then construct a residual-type a posteriori error estimator that explicitly incorporates the PML truncation error as well as the finite element discretization error. Utilizing the a posteriori error estimate, we propose an adaptive PML-FEM algorithm. Numerical experiments are also presented to demonstrate the effectiveness of the proposed adaptive algorithm, in particular for configurations with geometric singularities.

The remainder of this paper is organized as follows. In Section 2, we introduce the mathematical formulation of the acoustic-elastic interaction problem in periodic structures and the associated weak formulation. The truncated PML model and the convergence analysis of the PML approximation are presented in Section 3. Section 4 is devoted to the finite element discretization and the residual-based a posteriori error estimate. In Section 5, we describe the implementation of the adaptive algorithm and show numerical results. Conclusions and future extensions are given in Section 6.

2. Problem Formulation

In this section, we introduce the original model and its corresponding weak formulation of the acoustic-elastic interaction problem in periodic structures.

2.1. Original model

Assume that the surface of the elastic solid is periodic in the x_1 -axis with the period Λ . Due to the periodic structure of the elastic body, the problem can be restricted into a single periodic cell, where $x_1 \in (0, \Lambda)$. Denote the surface of the elastic body by

$$\Gamma = \{ \mathbf{x} = (x_1, x_2) \in \mathbb{R}^2 : x_1 \in (0, \Lambda), x_2 = f(x_1) \},$$

where f is a Lipschitz function with period $\Lambda > 0$. Denote by

$$\Omega_u = \{ \mathbf{x} \in \mathbb{R}^2 : x_1 \in (0, \Lambda), x_2 > f(x_1) \}$$

the domain above the periodic surface, which is filled with a homogeneous compressible inviscid fluid with a constant mass density $\rho_f > 0$. The domain below the surface is denoted by

$$\Omega_d = \{ \mathbf{x} \in \mathbb{R}^2 : x_1 \in (0, \Lambda), x_2 < f(x_1) \},$$

which is occupied by an isotropic homogeneous elastic solid body characterized by the mass density $\rho > 0$ and the Lamé constants $\lambda, \mu \in \mathbb{R}$ satisfying $\mu > 0$ and $\lambda + \mu > 0$. Define the artificial boundaries above and below the fluid-solid interface as $\Gamma_+ = \{ \mathbf{x} \in \mathbb{R}^2 : x_1 \in (0, \Lambda), x_2 = h_1 \}$ and $\Gamma_- = \{ \mathbf{x} \in \mathbb{R}^2 : x_1 \in (0, \Lambda), x_2 = h_2 \}$, where h_1 and h_2 are constants. Let

$$\begin{aligned} \Omega_+ &= \{ \mathbf{x} \in \mathbb{R}^2 : x_1 \in (0, \Lambda), f(x_1) < x_2 < h_1 \}, \\ \Omega_- &= \{ \mathbf{x} \in \mathbb{R}^2 : x_1 \in (0, \Lambda), h_2 < x_2 < f(x_1) \}. \end{aligned}$$

Similarly, we define

$$\begin{aligned} \Omega_+^e &= \{ \mathbf{x} \in \mathbb{R}^2 : x_1 \in (0, \Lambda), x_2 > h_1 \}, \\ \Omega_-^e &= \{ \mathbf{x} \in \mathbb{R}^2 : x_1 \in (0, \Lambda), x_2 < h_2 \}. \end{aligned}$$

Fig. 1 shows the problem geometry of acoustic-elastic interaction in periodic structures. Let $\mathbf{n} = (n_1, n_2)^\top$ be the unit normal vector to Γ directed into Ω_u , and denote $\Omega = \Omega_+ \cup \Omega_-$.

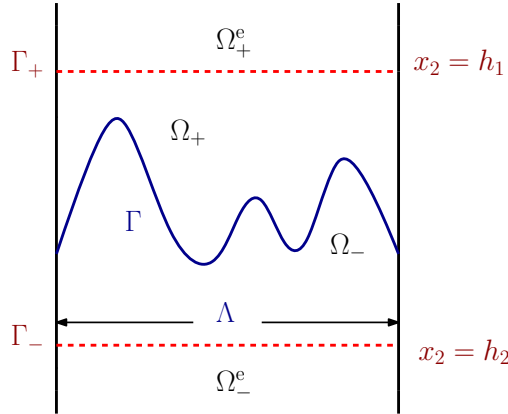


Figure 1: Problem geometry of acoustic-elastic interaction in periodic structures.

Let $p^{\text{in}} = e^{i(\alpha x_1 - \beta x_2)}$ be the incoming acoustic wave, where $\alpha = \kappa \sin \theta, \beta = \kappa \cos \theta$, and $\theta \in (-\pi/2, \pi/2)$ is the incident angle. When the plane wave incident onto the elastic surface, the scattered acoustic wave p^{sc} in the fluid domain and the transmitted elastic wave $\mathbf{u} = (u_1, u_2)^\top$ in the solid domain are excited at the same time, where p^{sc} satisfies the Helmholtz equation

$$\Delta p^{\text{sc}} + \kappa^2 p^{\text{sc}} = 0 \quad \text{in } \Omega_u,$$

while \mathbf{u} admits the Naiver equation

$$\Delta^* \mathbf{u} + \omega^2 \rho \mathbf{u} = 0 \quad \text{in } \Omega_d. \quad (1)$$

Here, κ is the wavenumber, $\omega > 0$ is the angular frequency, and $\Delta^* := \mu \Delta + (\lambda + \mu) \nabla \nabla \cdot$. To ensure the continuity of the normal component of the velocity, the kinematic interface condition

$$\partial_{\mathbf{n}}(p^{\text{in}} + p^{\text{sc}}) = \rho_f \omega^2 \mathbf{u} \cdot \mathbf{n} \quad \text{on } \Gamma$$

is required. In addition, the following dynamic interface condition

$$-(p^{\text{in}} + p^{\text{sc}})\mathbf{n} = \mathbf{T}\mathbf{u} \quad \text{on } \Gamma$$

is imposed to ensure the continuity of the traction (cf. [41, 50, 51]). Here, the traction of \mathbf{u} is defined by

$$\mathbf{T}\mathbf{u} := 2\mu\partial_{\mathbf{v}}\mathbf{u} + \lambda\mathbf{v}\nabla \cdot \mathbf{u} - \mu \begin{bmatrix} \left(\frac{\partial u_1}{\partial x_2} - \frac{\partial u_2}{\partial x_1}\right)v_2 \\ \left(\frac{\partial u_2}{\partial x_1} - \frac{\partial u_1}{\partial x_2}\right)v_1 \end{bmatrix}, \quad (2)$$

where $\mathbf{v} = (v_1, v_2)^{\top}$ is the unit normal vector of Ω_- . We want to reduce the original problem equivalently to a boundary value problem in Ω . To this end, we introduce exact transparent boundary conditions for acoustic and elastic waves defined on Γ_+ and Γ_- , respectively.

Let $H^1(\Omega_+)$ and $H^1(\Omega_-)$ be the standard Sobolev spaces. The corresponding quasi-periodic functional spaces are defined by

$$\begin{aligned} H_{\text{qp}}^1(\Omega_+) &:= \left\{ p \in H^1(\Omega_+) : p(\Lambda, x_2) = p(0, x_2) e^{i\alpha\Lambda} \right\}, \\ H_{\text{qp}}^1(\Omega_-) &:= \left\{ u \in H^1(\Omega_-) : u(\Lambda, x_2) = u(0, x_2) e^{i\alpha\Lambda} \right\}. \end{aligned}$$

Given any quasi-periodic function $p \in H_{\text{qp}}^1(\Omega_+)$, it admits a Fourier series expansion

$$p(x_1, x_2) = \sum_{n \in \mathbb{Z}} p_n(x_2) e^{i\alpha_n x_1}, \quad p_n(x_2) = \frac{1}{\Lambda} \int_0^\Lambda p(x_1, x_2) e^{-i\alpha_n x_1} dx_1,$$

where $\alpha_n = 2n\pi/\Lambda + \alpha$. For any $s \in \mathbb{R}$, the trace functional space $H^s(\Gamma_+)$ is defined by

$$H^s(\Gamma_+) = \left\{ p \in L^2(\Gamma_+) : \|p\|_{H^s(\Gamma_+)} < \infty \right\}$$

with the trace norm

$$\|p\|_{H^s(\Gamma_+)}^2 = \Lambda \sum_{n \in \mathbb{Z}} (1 + \alpha_n^2)^s |p_n(h_1)|^2.$$

Similarly, we can define the trace functional space $H^s(\Gamma_-)$ and the corresponding trace norm $\|\cdot\|_{H^s(\Gamma_-)}$. We firstly introduce the TBC of the scattered field p^{sc} . Note that the Rayleigh expansion (cf. [49]) of p^{sc} can be defined by

$$p^{\text{sc}}(x_1, x_2) = \sum_{n \in \mathbb{Z}} p_n^{\text{sc}}(h_1) e^{i(\alpha_n x_1 + \beta_n(x_2 - h_1))}, \quad x_2 > h_1, \quad (3)$$

where

$$\beta_n = \begin{cases} (\kappa^2 - \alpha_n^2)^{1/2}, & |\alpha_n| < \kappa, \\ i(\alpha_n^2 - \kappa^2)^{1/2}, & |\alpha_n| > \kappa. \end{cases}$$

We always assume that $\beta_n \neq 0$, i.e. $|\alpha_n| \neq \kappa$ to exclude Wood's anomalies [4]. Taking the normal derivative of (3) with respect to x_2 and then evaluating it at $x_2 = h_1$, one can get

$$\partial_{x_2} p^{\text{sc}}(x_1, h_1) = \sum_{n \in \mathbb{Z}} i\beta_n p_n^s(h_1) e^{i\alpha_n x_1}.$$

It was shown in [49] that for any quasi-periodic function p , the Dirichlet-to-Neumann (DtN) operator on Γ_+ is defined by

$$\mathcal{T}_+ p(x_1, h_1) := \sum_{n \in \mathbb{Z}} i\beta_n p_n(h_1) e^{i\alpha_n x_1}. \quad (4)$$

Based on (4), the TBC for the scattered field p^{sc} can be defined by

$$\partial_{x_2} p^{\text{sc}} = \mathcal{T}_+ p^{\text{sc}} \quad \text{on } \Gamma_+. \quad (5)$$

Next, we turn to derive the TBC for the transmitted field \mathbf{u} . Let the Jacobian matrix of \mathbf{u} be

$$\nabla \mathbf{u} = \begin{bmatrix} \partial_{x_1} u_1 & \partial_{x_2} u_1 \\ \partial_{x_1} u_2 & \partial_{x_2} u_2 \end{bmatrix}.$$

The operators **curl** and **curl** are defined respectively by

$$\text{curl } \mathbf{u} = \partial_{x_1} u_2 - \partial_{x_2} u_1, \quad \text{curl } \mathbf{u} = [\partial_{x_2} u, -\partial_{x_1} u]^\top.$$

The transmitted field \mathbf{u} in Ω_- can be decomposed into the compressional part \mathbf{u}_p and the shear part \mathbf{u}_s , i.e.,

$$\mathbf{u}_p = -\frac{1}{\kappa_1^2} \nabla \nabla \cdot \mathbf{u}, \quad \mathbf{u}_s = \frac{1}{\kappa_2^2} \text{curl curl } \mathbf{u},$$

where

$$\kappa_1 = \omega \sqrt{\frac{\rho}{2\mu + \lambda}}, \quad \kappa_2 = \omega \sqrt{\frac{\rho}{\mu}}$$

are called the compressional and shear wavenumbers satisfying $\kappa_2 > \kappa_1$. For any solution \mathbf{u} of (1), it satisfies the Helmholtz decomposition

$$\mathbf{u} = \nabla \phi_1 + \text{curl} \phi_2, \quad (6)$$

where ϕ_j ($j = 1, 2$) is called the scalar potential function. Combining (1) and (6) yields

$$\Delta \phi_j + \kappa_j^2 \phi_j = 0.$$

Due to the quasi-periodicity of \mathbf{u} , it follows from (6) that ϕ_j is also a quasi-periodic function in the x_1 direction with the period Λ and admits the following Rayleigh expansion

$$\phi_j(x_1, x_2) = \sum_{n \in \mathbb{Z}} \phi_n^{(j)}(h_2) e^{i(\alpha_n x_1 - \beta_n^{(j)}(x_2 - h_2))}, \quad x_2 < h_2,$$

where

$$\beta_n^{(j)} = \begin{cases} (\kappa_j^2 - \alpha_n^2)^{1/2}, & |\alpha_n| < \kappa_j, \\ i(\alpha_n^2 - \kappa_j^2)^{1/2}, & |\alpha_n| > \kappa_j. \end{cases}$$

Similarly, we assume that $\kappa_j \neq |\alpha_n|$. It has been shown in [39] that the transmitted field \mathbf{u} has the expansion

$$\begin{aligned} \mathbf{u}(x_1, x_2) &= \sum_{n \in \mathbb{Z}} \frac{1}{X_n} \begin{bmatrix} \alpha_n^2 & -\alpha_n \beta_n^{(2)} \\ -\alpha_n \beta_n^{(1)} & \beta_n^{(1)} \beta_n^{(2)} \end{bmatrix} \mathbf{u}_n(h_2) e^{i(\alpha_n x_1 - \beta_n^{(1)}(x_2 - h_2))} \\ &\quad + \frac{1}{X_n} \begin{bmatrix} \beta_n^{(1)} \beta_n^{(2)} & \alpha_n \beta_n^{(2)} \\ \alpha_n \beta_n^{(1)} & \alpha_n^2 \end{bmatrix} \mathbf{u}_n(h_2) e^{i(\alpha_n x_1 - \beta_n^{(2)}(x_2 - h_2))}, \quad x_2 < h_2, \end{aligned} \quad (7)$$

where $X_n = \alpha_n^2 + \beta_n^{(1)} \beta_n^{(2)}$. Based on (2), we can define the boundary operator on Γ_- as

$$\begin{aligned} \mathcal{T}_- \mathbf{u} &:= -2\mu \partial_{x_2} \mathbf{u} + \lambda [0, -1]^\top \nabla \cdot \mathbf{u} + \mu \begin{bmatrix} \frac{\partial u_1}{\partial x_2} - \frac{\partial u_2}{\partial x_1} \\ 0 \end{bmatrix} \\ &= \begin{bmatrix} -\mu \left(\frac{\partial u_1}{\partial x_2} + \frac{\partial u_2}{\partial x_1} \right) \\ -(2\mu + \lambda) \frac{\partial u_2}{\partial x_2} - \lambda \frac{\partial u_1}{\partial x_1} \end{bmatrix}. \end{aligned} \quad (8)$$

From (7) and (8), the TBC of the transmitted field \mathbf{u} is defined by

$$\mathcal{B}\mathbf{u} = \mathcal{T}_-\mathbf{u} = \sum_{n \in \mathbb{Z}} W_n \begin{bmatrix} u_n^{(1)}(h_2), u_n^{(2)}(h_2) \end{bmatrix}^\top e^{i\alpha_n x_1}, \quad (9)$$

where \mathcal{T}_- is the elastic DtN operator and the coefficient matrix is defined by

$$W_n = \frac{i}{X_n} \begin{bmatrix} \omega^2 \rho \beta_n^{(1)} & -2\mu \alpha_n X_n + \omega^2 \rho \alpha_n \\ 2\mu \alpha_n X_n - \omega^2 \rho \alpha_n & \omega^2 \rho \beta_n^{(2)} \end{bmatrix}.$$

Then by the above transparent boundary conditions, one can obtain an acoustic-elastic interaction boundary value problem in periodic structures: Given p^{in} , seek quasi-periodic solutions p^{sc} and \mathbf{u} such that

$$\begin{aligned} \Delta p^{\text{sc}} + \kappa^2 p^{\text{sc}} &= 0 && \text{in } \Omega_+, \\ \Delta^* \mathbf{u} + \omega^2 \rho \mathbf{u} &= 0 && \text{in } \Omega_-, \\ \partial_n(p^{\text{in}} + p^{\text{sc}}) &= \rho_f \omega^2 \mathbf{u} \cdot \mathbf{n} && \text{on } \Gamma, \\ -(p^{\text{in}} + p^{\text{sc}}) \mathbf{n} &= \mathbf{T} \mathbf{u} && \text{on } \Gamma, \\ \partial_{x_2} p^{\text{sc}} &= \mathcal{T}_+ p^{\text{sc}} && \text{on } \Gamma_+, \\ \mathcal{B}\mathbf{u} &= \mathcal{T}_- \mathbf{u} && \text{on } \Gamma_-. \end{aligned} \quad (10)$$

As shown in [25], we know that the uniqueness of the solution for a bounded elastic body does not hold at Jones frequencies. Therefore, throughout the paper, we assume that the frequency ω is not a Jones frequency.

2.2. Variational problem

In this subsection, we give the variational formulation of the acoustic-elastic interaction in periodic structures. To facilitate subsequent theoretical analysis, we introduce the following product Sobolev space

$$\mathcal{H}_{\text{qp}}^1(\Omega) := H_{\text{qp}}^1(\Omega_+) \times H_{\text{qp}}^1(\Omega_-)^2 = \left\{ \mathbf{U} = (p, \mathbf{u}) : p \in H_{\text{qp}}^1(\Omega_+), \mathbf{u} \in H_{\text{qp}}^1(\Omega_-)^2 \right\}.$$

The corresponding norm is defined by

$$\begin{aligned} \|V\|_{\mathcal{H}_{\text{qp}}^1(\Omega)}^2 &= (V, V)_{\mathcal{H}_{\text{qp}}^1(\Omega)} \\ &= \int_{\Omega_+} (\nabla \varphi \cdot \nabla \bar{\varphi} + \varphi \bar{\varphi}) \, dx + \int_{\Omega_-} (\mathcal{E}_{\lambda, \mu}(\psi, \bar{\psi}) + \psi \cdot \bar{\psi}) \, dx, \quad \forall V = (\varphi, \psi), \end{aligned}$$

where

$$\begin{aligned} \mathcal{E}_{\lambda, \mu}(\mathbf{u}, \psi) &= \lambda(\nabla \cdot \mathbf{u})(\nabla \cdot \bar{\psi}) + \frac{\mu}{2} \left(\nabla \mathbf{u} + \nabla \mathbf{u}^\top \right) : \left(\nabla \bar{\psi} + \nabla \bar{\psi}^\top \right) \\ &= (2\mu + \lambda) \left(\frac{\partial u_1}{\partial x_1} \frac{\partial \bar{\psi}_1}{\partial x_1} + \frac{\partial u_2}{\partial x_2} \frac{\partial \bar{\psi}_2}{\partial x_2} \right) + \mu \left(\frac{\partial u_1}{\partial x_2} \frac{\partial \bar{\psi}_1}{\partial x_2} + \frac{\partial u_2}{\partial x_1} \frac{\partial \bar{\psi}_2}{\partial x_1} \right) \\ &\quad + \lambda \left(\frac{\partial u_2}{\partial x_2} \frac{\partial \bar{\psi}_1}{\partial x_1} + \frac{\partial u_1}{\partial x_1} \frac{\partial \bar{\psi}_2}{\partial x_2} \right) + \mu \left(\frac{\partial u_2}{\partial x_1} \frac{\partial \bar{\psi}_1}{\partial x_2} + \frac{\partial u_1}{\partial x_2} \frac{\partial \bar{\psi}_2}{\partial x_1} \right). \end{aligned}$$

Note that $A : B = \text{tr}(AB^\top)$ is the Frobenius inner product of 2×2 matrices A and B . Besides, from the second Korn's inequality, it can be easily verified that $\|\cdot\|_{\mathcal{H}_{\text{qp}}^1(\Omega)}$ is equivalent to the standard H^1 -norm; see also [50].

By the Green's formula and the first Betti's formula, we can derive the weak formulation of the original problem (10): Given p^{in} , seek $\mathbf{U} = (p^{\text{sc}}, \mathbf{u}) \in \mathcal{H}_{\text{qp}}^1(\Omega)$ such that

$$A(\mathbf{U}, V) = L(V), \quad \forall V = (\varphi, \psi) \in \mathcal{H}_{\text{qp}}^1(\Omega). \quad (11)$$

Here, the sesquilinear form $A : \mathcal{H}_{qp}^1(\Omega) \times \mathcal{H}_{qp}^1(\Omega) \rightarrow \mathbb{C}$ is defined by

$$A(\mathbf{U}, \mathbf{V}) = \tilde{A}(\mathbf{U}, \mathbf{V}) + \tilde{B}_1(\mathbf{U}, \mathbf{V}) + \tilde{B}_2(\mathbf{U}, \mathbf{V}), \quad (12)$$

where

$$\begin{aligned} \tilde{A}(\mathbf{U}, \mathbf{V}) &= \int_{\Omega_+} (\nabla p^{sc} \cdot \nabla \bar{\varphi} - \kappa^2 p^{sc} \bar{\varphi}) \, dx + \int_{\Omega_-} (\mathcal{E}_{\lambda, \mu}(\mathbf{u}, \bar{\psi}) - \omega^2 \rho \mathbf{u} \cdot \bar{\psi}) \, dx, \\ \tilde{B}_1(\mathbf{U}, \mathbf{V}) &= \int_{\Gamma} p^{sc} \mathbf{n} \cdot \bar{\psi} \, ds + \int_{\Gamma} \rho_f \omega^2 \mathbf{u} \cdot \mathbf{n} \bar{\varphi} \, ds, \\ \tilde{B}_2(\mathbf{U}, \mathbf{V}) &= - \int_{\Gamma_+} \mathcal{T}_+ p^{sc} \bar{\varphi} \, ds - \int_{\Gamma_-} \mathcal{T}_- \mathbf{u} \cdot \bar{\psi} \, ds. \end{aligned}$$

The term L on the right-hand side of equation (11) is a bounded linear functional dependent on $(\partial_{\mathbf{n}} p^{in}, p^{in}) \in H^{-1/2}(\Gamma) \times H^{1/2}(\Gamma)$, which is defined by

$$L(\mathbf{V}) = \int_{\Gamma} \partial_{\mathbf{n}} p^{in} \bar{\varphi} - p^{in} \mathbf{n} \cdot \bar{\psi} \, ds. \quad (13)$$

We get from Lemma 4.1 in [25] that the sesquilinear form $A(\cdot, \cdot)$ satisfies Gårding's inequality. Besides, it has also been shown in [25] that the variational problem (11) has the unique solvability with Jones frequencies excluded. Then, it follows from the idea of [24] that the following inf-sup condition holds

$$\sup_{0 \neq \mathbf{V} \in \mathcal{H}_{qp}^1(\Omega)} \frac{|A(\mathbf{U}, \mathbf{V})|}{\|\mathbf{V}\|_{\mathcal{H}_{qp}^1(\Omega)}} \geq \gamma_0 \|\mathbf{U}\|_{\mathcal{H}_{qp}^1(\Omega)}, \quad \forall \mathbf{U} \in \mathcal{H}_{qp}^1(\Omega), \quad (14)$$

where $\gamma_0 > 0$ is a constant independent of \mathbf{U} .

3. PML Approximation

This section firstly focuses on constructing a truncated PML problem as an approximation to the original acoustic-elastic interaction in periodic structures, and then discusses the exponential convergence of the PML approximation error.

3.1. PML setting

We begin by introducing the absorbing PML media. Let the regions above Γ_+ and below Γ_- be filled with PML layers of thicknesses δ_1 and δ_2 , respectively. The acoustic and elastic PML domains are respectively denoted by

$$\begin{aligned} \Omega_+^{\text{PML}} &= \{ \mathbf{x} \in \mathbb{R}^2 : 0 < x_1 < \Lambda, h_1 < x_2 < h_1 + \delta_1 \}, \\ \Omega_-^{\text{PML}} &= \{ \mathbf{x} \in \mathbb{R}^2 : 0 < x_1 < \Lambda, h_2 - \delta_2 < x_2 < h_2 \}, \end{aligned}$$

with the corresponding acoustic and elastic PML boundaries

$$\begin{aligned} \Gamma_+^{\text{PML}} &= \{ \mathbf{x} \in \mathbb{R}^2 : 0 < x_1 < \Lambda, x_2 = h_1 + \delta_1 \}, \\ \Gamma_-^{\text{PML}} &= \{ \mathbf{x} \in \mathbb{R}^2 : 0 < x_1 < \Lambda, x_2 = h_2 - \delta_2 \}. \end{aligned}$$

Fig. 2 shows the problem geometry of acoustic-elastic interaction in periodic structures with PML layers. Let $s(\tau) = s_1(\tau) + is_2(\tau)$ be the continuous PML function satisfying

$$\begin{aligned} s(\tau) &= 1 \quad \text{for } h_2 < \tau < h_1, \\ s_1(\tau) &\geq 1, \quad s_2(\tau) > 0 \quad \text{otherwise.} \end{aligned}$$

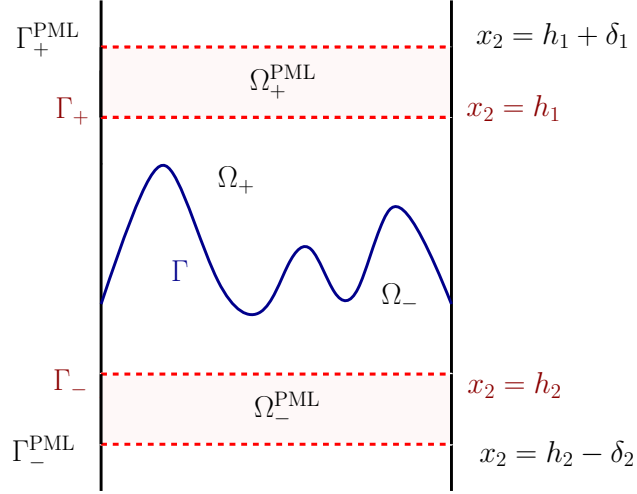


Figure 2: Problem geometry of acoustic-elastic interaction in periodic structures with PML layers.

Then the PML can be introduced by the following complex coordinate stretching

$$\hat{x}_2 = \int_0^{x_2} s(\tau) d\tau.$$

Obviously, we have $\nabla_{\hat{x}} = [\partial_{x_1}, \partial_{\hat{x}_2}]^T = [\partial_{x_1}, s^{-1} \partial_{x_2}]^T$, where $\hat{x} = (x_1, \hat{x}_2)^T$. In addition, we can obtain

$$\begin{aligned} \Delta_{\hat{x}} p^{\text{sc}}(\hat{x}) + \kappa^2 p^{\text{sc}}(\hat{x}) &= 0 & \text{in } \Omega_u, \\ \Delta_{\hat{x}}^* \mathbf{u}(\hat{x}) + \omega^2 \rho \mathbf{u}(\hat{x}) &= 0 & \text{in } \Omega_d, \end{aligned}$$

where

$$\Delta_{\hat{x}} = \nabla_{\hat{x}} \cdot \nabla_{\hat{x}}, \quad \Delta_{\hat{x}}^* = \mu \Delta_{\hat{x}} + (\lambda + \mu) \nabla_{\hat{x}} \nabla_{\hat{x}} \cdot.$$

Denote by

$$p^{\text{sc}}(\hat{x}) = p^{\text{sc}}(\hat{x}(x)) := \hat{p}^{\text{sc}}(x) \quad \text{and} \quad \mathbf{u}(\hat{x}) = \mathbf{u}(\hat{x}(x)) := \hat{\mathbf{u}}(x). \quad (15)$$

It is obvious that $\hat{p}^{\text{sc}}(x) = p^{\text{sc}}(x)$ in Ω_+ and $\hat{\mathbf{u}}(x) = \mathbf{u}(x)$ in Ω_- since $\hat{x} = x$ in $x_2 \in (h_2, h_1)$. Denote the respective acoustic and elastic PML equations by

$$\begin{aligned} \mathcal{L}_1 \hat{p}^{\text{sc}} &= 0 & \text{in } \Omega_+^{\text{PML}}, \\ \mathcal{L}_2 \hat{\mathbf{u}} &= 0 & \text{in } \Omega_-^{\text{PML}}. \end{aligned}$$

Here, the first operator \mathcal{L}_1 is defined by

$$\mathcal{L}_1 p := \nabla \cdot (\mathbb{A} \nabla p) + \kappa^2 s(x_2) p,$$

where

$$\mathbb{A}(x) = \begin{bmatrix} \mathbb{A}_{11} & 0 \\ 0 & \mathbb{A}_{22} \end{bmatrix} = \begin{bmatrix} s(x_2) & 0 \\ 0 & s^{-1}(x_2) \end{bmatrix}.$$

The second operator \mathcal{L}_2 is defined by

$$\mathcal{L}_2 \mathbf{u} := \begin{bmatrix} (2\mu + \lambda) \frac{\partial}{\partial x_1} \left(s(x_2) \frac{\partial u_1}{\partial x_1} \right) + \mu \frac{\partial}{\partial x_2} \left(s^{-1}(x_2) \frac{\partial u_1}{\partial x_2} \right) + (\lambda + \mu) \frac{\partial^2 u_1}{\partial x_1 \partial x_2} + \omega^2 \rho s(x_2) u_1 \\ (2\mu + \lambda) \frac{\partial}{\partial x_2} \left(s^{-1}(x_2) \frac{\partial u_2}{\partial x_2} \right) + \mu \frac{\partial}{\partial x_1} \left(s(x_2) \frac{\partial u_2}{\partial x_1} \right) + (\lambda + \mu) \frac{\partial^2 u_2}{\partial x_1 \partial x_2} + \omega^2 \rho s(x_2) u_2 \end{bmatrix}.$$

From equations (3), (7) and (15), we can conclude that \hat{p}^{sc} and $\hat{\mathbf{u}}$ exhibit exponential decay properties in Ω_+^{e} and Ω_-^{e} as $x_2 \rightarrow \infty$ and $x_2 \rightarrow -\infty$, respectively. Thus, it is reasonable to impose the homogeneous Dirichlet boundary conditions on boundaries Γ_+^{PML} and Γ_-^{PML} for the PML problem. Let $D_+ = \Omega_+ \cup \Omega_+^{\text{PML}} \cup \Gamma_+$ and $D_- = \Omega_- \cup \Omega_-^{\text{PML}} \cup \Gamma_-$. Then the truncated PML problem reads as: Given p^{in} , seek the quasi-periodic functions \hat{p}^{sc} and $\hat{\mathbf{u}}$ such that

$$\begin{aligned} \mathcal{L}_1 \hat{p}^{\text{sc}} &= 0 && \text{in } D_+, \\ \mathcal{L}_2 \hat{\mathbf{u}} &= 0 && \text{in } D_-, \\ \hat{p}^{\text{sc}} &= 0 && \text{on } \Gamma_+^{\text{PML}}, \\ \hat{\mathbf{u}} &= 0 && \text{on } \Gamma_-^{\text{PML}}, \\ \partial_{\mathbf{n}}(p^{\text{in}} + \hat{p}^{\text{sc}}) &= \rho_f \omega^2 \hat{\mathbf{u}} \cdot \mathbf{n} && \text{on } \Gamma, \\ -(p^{\text{in}} + \hat{p}^{\text{sc}}) \mathbf{n} &= \mathbf{T} \hat{\mathbf{u}} && \text{on } \Gamma. \end{aligned} \quad (16)$$

For convenience in defining the variational problem with respect to (16), we introduce the following Sobolev spaces

$$\begin{aligned} H_{0,\text{qp}}^1(D_+) &= \left\{ \varphi \in H_{\text{qp}}^1(D_+) : \varphi = 0 \text{ on } \Gamma_+^{\text{PML}} \right\}, \\ H_{0,\text{qp}}^1(D_-)^2 &= \left\{ \boldsymbol{\psi} \in H_{\text{qp}}^1(D_-)^2 : \boldsymbol{\psi} = 0 \text{ on } \Gamma_-^{\text{PML}} \right\}. \end{aligned}$$

Let $D = D_+ \cup D_-$, and define the product Sobolev space

$$\mathcal{H}_{0,\text{qp}}^1(D) := H_{0,\text{qp}}^1(D_+) \times H_{0,\text{qp}}^1(D_-)^2 = \left\{ \mathbf{V} = (\varphi, \boldsymbol{\psi}) : \varphi \in H_{0,\text{qp}}^1(D_+), \boldsymbol{\psi} \in H_{0,\text{qp}}^1(D_-)^2 \right\}.$$

Similarly, by combining the Green's formula and the first Betti's formula, we arrive at the variational formulation of (16): Given p^{in} , seek $\hat{\mathbf{U}} = (\hat{p}^{\text{sc}}, \hat{\mathbf{u}}) \in \mathcal{H}_{\text{qp}}^1(D)$ such that

$$B_D(\hat{\mathbf{U}}, \mathbf{V}) = L(\mathbf{V}), \quad \forall \mathbf{V} = (\varphi, \boldsymbol{\psi}) \in \mathcal{H}_{0,\text{qp}}^1(D). \quad (17)$$

For any $G_+ \subseteq D_+$ and $G_- \subseteq D_-$, we denote $G = G_+ \cup G_-$. Then the sesquilinear form $B_G : \mathcal{H}_{\text{qp}}^1(G) \times \mathcal{H}_{\text{qp}}^1(G) \rightarrow \mathbb{C}$ is defined by

$$B_G(\mathbf{U}, \mathbf{V}) = \tilde{B}_G(\mathbf{U}, \mathbf{V}) + \tilde{B}_1(\mathbf{U}, \mathbf{V}), \quad \forall \mathbf{U}, \mathbf{V} \in \mathcal{H}_{\text{qp}}^1(G), \quad (18)$$

where

$$\begin{aligned} \tilde{B}_G(\mathbf{U}, \mathbf{V}) &= \int_{G_+} \left(\mathbb{A} \nabla p^{\text{sc}} \cdot \nabla \bar{\varphi} - \kappa^2 s(x_2) p^{\text{sc}} \bar{\varphi} \right) dx + \int_{G_-} \left(\mathcal{S}_{\lambda,\mu}(\mathbf{u}, \boldsymbol{\psi}) - \omega^2 \rho s(x_2) \mathbf{u} \cdot \bar{\boldsymbol{\psi}} \right) dx, \\ \tilde{B}_1(\mathbf{U}, \mathbf{V}) &= \int_{\Gamma} p^{\text{sc}} \mathbf{n} \cdot \bar{\boldsymbol{\psi}} ds + \int_{\Gamma} \rho_f \omega^2 \mathbf{u} \cdot \bar{\mathbf{n}} \bar{\varphi} ds \end{aligned}$$

with

$$\begin{aligned} \mathcal{S}_{\lambda,\mu}(\mathbf{u}, \boldsymbol{\psi}) &= (2\mu + \lambda) \left(s(x_2) \frac{\partial u_1}{\partial x_1} \frac{\partial \bar{\psi}_1}{\partial x_1} + s^{-1}(x_2) \frac{\partial u_2}{\partial x_2} \frac{\partial \bar{\psi}_2}{\partial x_2} \right) + \mu \left(s^{-1}(x_2) \frac{\partial u_1}{\partial x_2} \frac{\partial \bar{\psi}_1}{\partial x_2} + s(x_2) \frac{\partial u_2}{\partial x_1} \frac{\partial \bar{\psi}_2}{\partial x_1} \right) \\ &\quad + \lambda \left(\frac{\partial u_2}{\partial x_2} \frac{\partial \bar{\psi}_1}{\partial x_1} + \frac{\partial u_1}{\partial x_1} \frac{\partial \bar{\psi}_2}{\partial x_2} \right) + \mu \left(\frac{\partial u_2}{\partial x_1} \frac{\partial \bar{\psi}_1}{\partial x_2} + \frac{\partial u_1}{\partial x_2} \frac{\partial \bar{\psi}_2}{\partial x_1} \right). \end{aligned}$$

3.2. TBCs of PML model

In this subsection, we aim to reformulate the problem (17) defined in D into an equivalent weak formulation defined in Ω by introducing TBCs for the truncated PML model. Let

$$\eta_1 = \int_{h_1}^{h_1 + \delta_1} s(\tau) d\tau, \quad \eta_2 = \int_{h_2 - \delta_2}^{h_2} s(\tau) d\tau. \quad (19)$$

In the complex coordinate, we have

$$\Delta_{\hat{x}} \hat{p}^{\text{sc}} + \kappa^2 \hat{p}^{\text{sc}} = 0 \quad \text{in } \Omega_+^{\text{PML}}, \quad (20)$$

$$\Delta_{\hat{x}}^* \hat{u} + \omega^2 \rho \hat{u} = 0 \quad \text{in } \Omega_-^{\text{PML}}. \quad (21)$$

From [16], the TBC on Γ_+ of the PML problem is defined by

$$\mathcal{T}_+^{\text{PML}} \hat{p}^{\text{sc}} := \sum_{n \in \mathbb{Z}} i\beta_n \coth(-i\beta_n \eta_1) \hat{p}_n^{\text{sc}}(h_1) e^{i\alpha_n x_1}, \quad (22)$$

where $\coth(y) = (e^y + e^{-y}) / (e^y - e^{-y})$. Next we turn to the derivation of the TBC defined on Γ_- . As is known, the solution of (21) admits the Helmholtz decomposition

$$\hat{u} = \nabla_{\hat{x}} \hat{\phi}_1 + \mathbf{curl}_{\hat{x}} \hat{\phi}_2, \quad (23)$$

where $\mathbf{curl}_{\hat{x}} = [\partial_{\hat{x}_2}, -\partial_{x_1}]^\top$. Since the solution \hat{u} is quasi-periodic, the function $\hat{\phi}_j(\hat{x}) = \phi_j(\hat{x})$, $j = 1, 2$ satisfies the Helmholtz equation

$$\Delta_{\hat{x}} \hat{\phi}_j + \kappa_j^2 \hat{\phi}_j = 0 \quad (24)$$

with the following Fourier series expansion

$$\hat{\phi}_j(x_1, x_2) = \sum_{n \in \mathbb{Z}} \hat{\phi}_n^{(j)}(x_2) e^{i\alpha_n x_1}. \quad (25)$$

Combining (24) and (25) gives

$$s^{-1}(x_2) \frac{d}{dx_2} \left(s^{-1}(x_2) \frac{d}{dx_2} \hat{\phi}_n^{(j)}(x_2) \right) + (\beta_n^{(j)})^2 \hat{\phi}_n^{(j)}(x_2) = 0,$$

whose general solution is given by

$$\hat{\phi}_n^{(j)}(x_2) = M_n^{(j)} e^{i\beta_n^{(j)} \int_{x_2}^{h_2} s(\tau) d\tau} + N_n^{(j)} e^{-i\beta_n^{(j)} \int_{x_2}^{h_2} s(\tau) d\tau}. \quad (26)$$

By using equations (23), (25), (26) and the homogeneous Dirichlet boundary condition

$$\hat{u}(x_1, h_2 - \delta_2) = 0 \quad \text{on } \Gamma_-^{\text{PML}},$$

we can see that the coefficients $M_n^{(j)}$ and $N_n^{(j)}$ satisfy the linear equations

$$\begin{bmatrix} \alpha_n & \alpha_n & -\beta_n^{(2)} & \beta_n^{(2)} \\ -\beta_n^{(1)} & \beta_n^{(1)} & -\alpha_n & -\alpha_n \\ \alpha_n e^{i\beta_n^{(1)} \eta_2} & \alpha_n e^{-i\beta_n^{(1)} \eta_2} & -\beta_n^{(2)} e^{i\beta_n^{(2)} \eta_2} & \beta_n^{(2)} e^{-i\beta_n^{(2)} \eta_2} \\ -\beta_n^{(1)} e^{i\beta_n^{(1)} \eta_2} & \beta_n^{(1)} e^{-i\beta_n^{(1)} \eta_2} & -\alpha_n e^{i\beta_n^{(2)} \eta_2} & -\alpha_n e^{-i\beta_n^{(2)} \eta_2} \end{bmatrix} \begin{bmatrix} M_n^{(1)} \\ N_n^{(1)} \\ M_n^{(2)} \\ N_n^{(2)} \end{bmatrix} = \begin{bmatrix} -i\hat{u}_n^{(1)}(h_2) \\ -i\hat{u}_n^{(2)}(h_2) \\ 0 \\ 0 \end{bmatrix}.$$

By solving the above linear equations, one has

$$\begin{aligned}
M_n^{(1)} &= \frac{i}{\mathcal{X}_n \hat{\mathcal{X}}_n} \left\{ -\frac{\mathcal{X}_n}{2} \left(\varsigma_n^{(1)} + 2 \right) \left(\alpha_n \hat{u}_n^{(1)}(h_2) - \beta_n^{(2)} \hat{u}_n^{(2)}(h_2) \right) \right. \\
&\quad \left. + \left(\varsigma_n^{(1)} + 2\xi_n^{(1)} \right) \left(\xi_n^{(2)} - \vartheta_n + 1 \right) \left(\alpha_n \beta_n^{(1)} \beta_n^{(2)} \hat{u}_n^{(1)}(h_2) - \alpha_n^2 \beta_n^{(2)} \hat{u}_n^{(2)}(h_2) \right) \right\}, \\
N_n^{(1)} &= \frac{i}{\mathcal{X}_n \hat{\mathcal{X}}_n} \left\{ \frac{\mathcal{X}_n \varsigma_n^{(1)}}{2} \left(\alpha_n \hat{u}_n^{(1)}(h_2) + \beta_n^{(2)} \hat{u}_n^{(2)}(h_2) \right) \right. \\
&\quad \left. + \left(\varsigma_n^{(1)} \xi_n^{(2)} + 2\xi_n^{(1)} \xi_n^{(2)} + 2\xi_n^{(1)} \right) \left(\alpha_n \beta_n^{(1)} \beta_n^{(2)} \hat{u}_n^{(1)}(h_2) + \alpha_n^2 \beta_n^{(2)} \hat{u}_n^{(2)}(h_2) \right) \right\}, \\
M_n^{(2)} &= \frac{i}{\mathcal{X}_n \hat{\mathcal{X}}_n} \left\{ \frac{\mathcal{X}_n}{2} \left[\varsigma_n^{(1)} \vartheta_n - 2 \left(\varsigma_n^{(1)} + 1 \right) \left(\xi_n^{(2)} + 1 \right) \right] \left(-\beta_n^{(1)} \hat{u}_n^{(1)}(h_2) - \alpha_n \hat{u}_n^{(2)}(h_2) \right) \right. \\
&\quad \left. + \varsigma_n^{(1)} \left(\xi_n^{(2)} - \vartheta_n + 1 \right) \left(-\left(\beta_n^{(1)} \right)^2 \beta_n^{(2)} \hat{u}_n^{(1)}(h_2) - \alpha_n^3 \hat{u}_n^{(2)}(h_2) \right) \right\}, \\
N_n^{(2)} &= \frac{i}{\mathcal{X}_n \hat{\mathcal{X}}_n} \left\{ \frac{\mathcal{X}_n}{2} \left[2\xi_n^{(2)} \left(\varsigma_n^{(1)} + 1 \right) - \varsigma_n^{(1)} \vartheta_n \right] \left(-\beta_n^{(1)} \hat{u}_n^{(1)}(h_2) + \alpha_n \hat{u}_n^{(2)}(h_2) \right) \right. \\
&\quad \left. - \xi_n^{(2)} \left(\varsigma_n^{(1)} + 2 \right) \left(-\left(\beta_n^{(1)} \right)^2 \beta_n^{(2)} \hat{u}_n^{(1)}(h_2) + \alpha_n^3 \hat{u}_n^{(2)}(h_2) \right) \right\},
\end{aligned}$$

where

$$\begin{aligned}
\varsigma_n^{(j)} &= \coth \left(-i\beta_n^{(j)} \eta_2 \right) - 1, \\
\xi_n^{(j)} &= \left(e^{i\beta_n^{(2)} \eta_2} - e^{i\beta_n^{(1)} \eta_2} \right) / \left(e^{-i\beta_n^{(j)} \eta_2} - e^{i\beta_n^{(j)} \eta_2} \right), \\
\vartheta_n &= \left(e^{-i\beta_n^{(1)} \eta_2} - e^{i\beta_n^{(1)} \eta_2} \right) / \left(e^{-i\beta_n^{(2)} \eta_2} - e^{i\beta_n^{(2)} \eta_2} \right), \\
\hat{\mathcal{X}}_n &= \mathcal{X}_n + 4\alpha_n^2 \beta_n^{(1)} \beta_n^{(2)} \left(\xi_n^{(2)} - \xi_n^{(1)} - \xi_n^{(1)} \xi_n^{(2)} \right) / \mathcal{X}_n.
\end{aligned}$$

It follows from (23) that

$$\begin{aligned}
\hat{\mathbf{u}}(x_1, x_2) &= i \sum_{n \in \mathbb{Z}} \left[\begin{array}{c} \alpha_n \\ -\beta_n^{(1)} \end{array} \right] M_n^{(1)} e^{i(\alpha_n x_1 + \beta_n^{(1)} \int_{x_2}^{h_2} s(\tau) d\tau)} + \left[\begin{array}{c} \alpha_n \\ \beta_n^{(1)} \end{array} \right] N_n^{(1)} e^{i(\alpha_n x_1 - \beta_n^{(1)} \int_{x_2}^{h_2} s(\tau) d\tau)} \\
&\quad - \left[\begin{array}{c} \beta_n^{(2)} \\ \alpha_n \end{array} \right] M_n^{(2)} e^{i(\alpha_n x_1 + \beta_n^{(2)} \int_{x_2}^{h_2} s(\tau) d\tau)} + \left[\begin{array}{c} \beta_n^{(2)} \\ -\alpha_n \end{array} \right] N_n^{(2)} e^{i(\alpha_n x_1 - \beta_n^{(2)} \int_{x_2}^{h_2} s(\tau) d\tau)}.
\end{aligned} \tag{27}$$

Using (8) and (27) yields the TBC for the transmitted field $\hat{\mathbf{u}}$ as

$$\mathcal{B}\hat{\mathbf{u}} = \mathcal{T}_-^{\text{PML}} \hat{\mathbf{u}} := \sum_{n \in \mathbb{Z}} \hat{W}^{(n)} \hat{\mathbf{u}}_n(h_2) e^{i\alpha_n x_1}, \tag{28}$$

where $\hat{W}^{(n)} = \begin{bmatrix} \hat{w}_{11}^{(n)} & \hat{w}_{12}^{(n)} \\ \hat{w}_{21}^{(n)} & \hat{w}_{22}^{(n)} \end{bmatrix}$ is a 2×2 matrix with entries defined by

$$\begin{aligned}
\hat{w}_{11}^{(n)} &= \frac{i}{\mathcal{X}_n \hat{\mathcal{X}}_n} \left\{ \omega^2 \rho \beta_n^{(1)} \mathcal{X}_n + \omega^2 \rho \beta_n^{(1)} \left[\varsigma_n^{(1)} \alpha_n^2 + \left(\varsigma_n^{(1)} \vartheta_n + 2\xi_n^{(2)} \right) \beta_n^{(1)} \beta_n^{(2)} \right] \right\}, \\
\hat{w}_{12}^{(n)} &= \frac{i\alpha_n}{\mathcal{X}_n \hat{\mathcal{X}}_n} \left\{ -2\mu \mathcal{X}_n \hat{\mathcal{X}}_n + \omega^2 \rho \mathcal{X}_n + \omega^2 \rho \beta_n^{(1)} \beta_n^{(2)} \left[\varsigma_n^{(1)} \left(2\xi_n^{(2)} - \vartheta_n + 1 \right) + 2\xi_n^{(2)} \right] \right\}, \\
\hat{w}_{21}^{(n)} &= \frac{i\alpha_n}{\mathcal{X}_n \hat{\mathcal{X}}_n} \left\{ 2\mu \mathcal{X}_n \hat{\mathcal{X}}_n - \omega^2 \rho \mathcal{X}_n + \omega^2 \rho \beta_n^{(1)} \beta_n^{(2)} \left[\varsigma_n^{(1)} \left(2\xi_n^{(2)} - \vartheta_n + 1 \right) + 4\xi_n^{(1)} \left(\xi_n^{(2)} + 1 \right) - 2\xi_n^{(2)} \right] \right\}, \\
\hat{w}_{22}^{(n)} &= \frac{i}{\mathcal{X}_n \hat{\mathcal{X}}_n} \left\{ \omega^2 \rho \beta_n^{(2)} \mathcal{X}_n + \omega^2 \rho \beta_n^{(2)} \left[\left(\varsigma_n^{(1)} \vartheta_n + 2\xi_n^{(2)} \right) \alpha_n^2 + \varsigma_n^{(1)} \beta_n^{(1)} \beta_n^{(2)} \right] \right\}.
\end{aligned}$$

Based on (22) and (28), we can reduce the PML model (16) to an equivalent boundary value problem: Given p^{in} , seek the quasi-periodic functions $p^{\text{sc,PML}}$ and \mathbf{u}^{PML} such that

$$\begin{aligned} \Delta p^{\text{sc,PML}} + \kappa^2 p^{\text{sc,PML}} &= 0 & \text{in } \Omega_+, \\ \Delta^* \mathbf{u}^{\text{PML}} + \omega^2 \rho \mathbf{u}^{\text{PML}} &= 0 & \text{in } \Omega_-, \\ \partial_n(p^{\text{in}} + p^{\text{sc,PML}}) &= \rho_f \omega^2 \mathbf{u}^{\text{PML}} \cdot \mathbf{n} & \text{on } \Gamma, \\ -(p^{\text{in}} + p^{\text{sc,PML}}) \mathbf{n} &= \mathbf{T} \mathbf{u}^{\text{PML}} & \text{on } \Gamma, \\ \partial_{x_2} p^{\text{sc,PML}} &= \mathcal{T}_+^{\text{PML}} p^{\text{sc,PML}} & \text{on } \Gamma_+, \\ \mathcal{B} \mathbf{u}^{\text{PML}} &= \mathcal{T}_-^{\text{PML}} \mathbf{u}^{\text{PML}} & \text{on } \Gamma_-. \end{aligned} \quad (29)$$

Besides, the variational formulation of the problem (29) reads as: Given p^{in} , seek $\mathbf{U}^{\text{PML}} = (p^{\text{sc,PML}}, \mathbf{u}^{\text{PML}}) \in \mathcal{H}_{\text{qp}}^1(\Omega)$ such that

$$A^{\text{PML}}(\mathbf{U}^{\text{PML}}, \mathbf{V}) = L(\mathbf{V}), \quad \forall \mathbf{V} = (\varphi, \psi) \in \mathcal{H}_{\text{qp}}^1(\Omega), \quad (30)$$

where

$$A^{\text{PML}}(\mathbf{U}^{\text{PML}}, \mathbf{V}) = \tilde{A}^{\text{PML}}(\mathbf{U}^{\text{PML}}, \mathbf{V}) + \tilde{B}_1^{\text{PML}}(\mathbf{U}^{\text{PML}}, \mathbf{V}) + \tilde{B}_2^{\text{PML}}(\mathbf{U}^{\text{PML}}, \mathbf{V}) \quad (31)$$

with

$$\begin{aligned} \tilde{A}^{\text{PML}}(\mathbf{U}^{\text{PML}}, \mathbf{V}) &= \int_{\Omega_+} (\nabla p^{\text{sc,PML}} \cdot \nabla \bar{\varphi} - \kappa^2 p^{\text{sc,PML}} \bar{\varphi}) \, dx + \int_{\Omega_-} (\mathcal{E}_{\lambda, \mu}(\mathbf{u}^{\text{PML}}, \mathbf{v}) - \omega^2 \rho \mathbf{u}^{\text{PML}} \cdot \bar{\psi}) \, dx, \\ \tilde{B}_1^{\text{PML}}(\mathbf{U}^{\text{PML}}, \mathbf{V}) &= \int_{\Gamma} \rho_f \omega^2 \mathbf{u}^{\text{PML}} \cdot \mathbf{n} \bar{\varphi} \, ds + \int_{\Gamma} p^{\text{sc,PML}} \mathbf{n} \cdot \bar{\psi} \, ds, \\ \tilde{B}_2^{\text{PML}}(\mathbf{U}^{\text{PML}}, \mathbf{V}) &= - \int_{\Gamma_+} \mathcal{T}_+^{\text{PML}} p^{\text{sc,PML}} \bar{\varphi} \, ds - \int_{\Gamma_-} \mathcal{T}_-^{\text{PML}} \mathbf{u}^{\text{PML}} \cdot \bar{\psi} \, ds. \end{aligned}$$

The relationship between the variational formulations (17) and (30) can be established via the following lemma. The proof is direct based on our constructions of TBCs for the PML model. For brevity, we omit the detailed steps here.

Lemma 1. *Any solution $\hat{\mathbf{U}}$ of (17) restricted to the domain Ω is a solution of (30). Conversely, any solution \mathbf{U}^{PML} of (30) can be uniquely extended to the region \mathbf{D} to be a solution $\hat{\mathbf{U}}$ of (17).*

3.3. Error analysis of PML approximation

In this subsection, we mainly focus on estimating the error between \mathbf{U}^{PML} and \mathbf{U} . To begin with, we introduce some notations for facilitating the subsequent theoretical analysis.

For the upper region, let $\Theta_n = |\kappa^2 - \alpha_n^2|^{1/2}$ and $I = \{n : |\alpha_n| < \kappa\}$. Then we obtain $\beta_n = \Theta_n$ for $n \in I$, and $\beta_n = \mathbf{i} \Theta_n$ for $n \notin I$. Similarly, for the lower region, define $\Theta_n^{(j)} = |\kappa_j^2 - \alpha_n^2|^{1/2}$ and $I_j = \{n : |\alpha_n| < \kappa_j\}$, $j = 1, 2$. Clearly, we have $\beta_n^{(j)} = \Theta_n^{(j)}$ for $n \in I_j$, and $\beta_n^{(j)} = \mathbf{i} \Theta_n^{(j)}$ for $n \notin I_j$. Denote by

$$\begin{aligned} \Theta^i &= \min \{\Theta_n : n \in I\}, \quad \Theta^e = \min \{\Theta_n : n \notin I\}, \\ \Theta_j^i &= \min \{\Theta_n^{(j)} : n \in I_j\}, \quad \Theta_j^e = \min \{\Theta_n^{(j)} : n \notin I_j\}. \end{aligned}$$

The following Lemma is the result about the trace theorem.

Lemma 2 (See [16, 30]). *For any $\varphi \in H_{\text{qp}}^1(\Omega_+)$, $\psi \in H_{\text{qp}}^1(\Omega_-)^2$, one has*

$$\begin{aligned} \|\varphi\|_{L^2(\Gamma_+)} &\leq \|\varphi\|_{H^{1/2}(\Gamma_+)} \leq \gamma_1 \|\varphi\|_{H^1(\Omega_+)}, \\ \|\psi\|_{L^2(\Gamma_-)^2} &\leq \|\psi\|_{H^{1/2}(\Gamma_-)^2} \leq \gamma_1 \|\psi\|_{H^1(\Omega_-)^2}, \end{aligned}$$

where $\gamma_1 = (1 + (h_1 - h_2)^{-1})^{1/2}$.

The Lemma 3 provides the error estimate between $\mathcal{T}_m^{\text{PML}}$ and \mathcal{T}_m ($m = +, -$).

Lemma 3. For any $(p, \mathbf{u}) \in \mathcal{H}_{\text{qp}}^1(\Omega)$, $(\varphi, \psi) \in \mathcal{H}_{\text{qp}}^1(\Omega)$, we obtain

$$\left| \langle (\mathcal{T}_+^{\text{PML}} - \mathcal{T}_+) p, \varphi \rangle_{\Gamma_+} \right| \leq F_1 \|p\|_{L^2(\Gamma_+)} \|\varphi\|_{L^2(\Gamma_+)}, \quad (32)$$

$$\left| \langle (\mathcal{T}_-^{\text{PML}} - \mathcal{T}_-) \mathbf{u}, \psi \rangle_{\Gamma_-} \right| \leq F_2 \|\mathbf{u}\|_{L^2(\Gamma_-)^2} \|\psi\|_{L^2(\Gamma_-)^2}, \quad (33)$$

where

$$F_1 = \max \left\{ \frac{2\Theta^i}{e^{2\Im\eta_1\Theta^i} - 1}, \frac{2\Theta^e}{e^{2\Re\eta_1\Theta^e} - 1} \right\}$$

and

$$F_2 = \frac{34\omega^2\rho}{\kappa_1^4} \times \max_{j=1,2} \left\{ \frac{\Theta_j^i}{e^{\frac{1}{2}\Theta_j^i\Im\eta_2} - 1}, \frac{\Theta_j^e}{e^{\frac{1}{2}\Theta_j^e\Re\eta_2} - 1} \right\} \times \max \left\{ 6\kappa_2, \kappa_2^2 + 4, 8\kappa_2^4, \frac{8\kappa_2^3}{\kappa_1^2}, \frac{12(\kappa_2^2 + 16)^2}{\kappa_1^2} \right\}.$$

Proof. The derivation of (32) is provided in [16, Lemma 2.2], and inequality (33) follows by an argument analogous to [30, Lemma 3.2]. Details are omitted here for brief. \square

In subsequent theoretical analysis, we always take the medium function $s(x_2)$ as

$$\begin{aligned} s(x_2) &= 1 + \sigma_1 \left(\frac{x_2 - h_1}{\delta_1} \right)^t, & \text{if } x_2 \geq h_1, \quad t \geq 1, \\ s(x_2) &= 1 + \sigma_2 \left(\frac{h_2 - x_2}{\delta_2} \right)^t, & \text{if } x_2 \leq h_2, \quad t \geq 1. \end{aligned}$$

Based on the definition of η_j ($j = 1, 2$) given by (19), a straightforward calculation shows

$$\Re\eta_j = \left(1 + \frac{\Re\sigma_j}{t+1} \right) \delta_j, \quad \Im\eta_j = \left(\frac{\Im\sigma_j}{t+1} \right) \delta_j.$$

which further implies that both $\Re\eta_j$ and $\Im\eta_j$ are determined by the PML parameters σ_j and δ_j . As is shown in Lemma 3, the errors associated with the boundary operators decay exponentially with respect to the PML parameters.

We are now ready to estimate the error between the solution of the PML problem and that of the original problem.

Theorem 1. Let \mathbf{U} and \mathbf{U}^{PML} be respective solutions to (11) and (30). If $\tilde{F}\gamma_1^2 < \gamma_0$, then the truncated PML problem (30) has a unique solution \mathbf{U}^{PML} , which satisfies the following error estimate:

$$\begin{aligned} \|\mathbf{U} - \mathbf{U}^{\text{PML}}\|_{\mathcal{H}_{\text{qp}}^1(\Omega)} &:= \sup_{0 \neq \mathbf{V} \in \mathcal{H}_{\text{qp}}^1(\Omega)} \frac{|A(\mathbf{U} - \mathbf{U}^{\text{PML}}, \mathbf{V})|}{\|\mathbf{V}\|_{\mathcal{H}_{\text{qp}}^1(\Omega)}} \\ &\leq F_1 \gamma_1 \|p^{\text{sc}, \text{PML}}\|_{L^2(\Gamma_+)} + F_2 \gamma_1 \|\mathbf{u}^{\text{PML}}\|_{L^2(\Gamma_-)^2}, \end{aligned} \quad (34)$$

where $\tilde{F} = \max\{F_1, F_2\}$, and the constants γ_0, γ_1 are respectively presented in (14) and Lemma 2.

Proof. In order to demonstrate that the variational problem (30) has a unique weak solution, we only need to establish the coercivity of the sesquilinear form A^{PML} in (31). Based on the definition of $A(\cdot, \cdot)$ and $A^{\text{PML}}(\cdot, \cdot)$, Lemmas 2 and 3, we have

$$\begin{aligned} |A^{\text{PML}}(\mathbf{U}, \mathbf{V})| &\geq |A(\mathbf{U}, \mathbf{V})| - \left| \langle (\mathcal{T}_+^{\text{PML}} - \mathcal{T}_+) p^{\text{sc}}, \varphi \rangle_{\Gamma_+} \right| - \left| \langle (\mathcal{T}_-^{\text{PML}} - \mathcal{T}_-) \mathbf{u}, \psi \rangle_{\Gamma_-} \right| \\ &\geq |A(\mathbf{U}, \mathbf{V})| - F_1 \|p^{\text{sc}}\|_{L^2(\Gamma_+)} \|\varphi\|_{L^2(\Gamma_+)} - F_2 \|\mathbf{u}\|_{L^2(\Gamma_-)^2} \|\psi\|_{L^2(\Gamma_-)^2} \\ &\geq |A(\mathbf{U}, \mathbf{V})| - F_1 \gamma_1^2 \|p^{\text{sc}}\|_{H^1(\Omega_+)} \|\varphi\|_{H^1(\Omega_+)} - F_2 \gamma_1^2 \|\mathbf{u}\|_{H^1(\Omega_-)^2} \|\psi\|_{H^1(\Omega_-)^2} \\ &\geq |A(\mathbf{U}, \mathbf{V})| - \tilde{F} \gamma_1^2 \|\mathbf{U}\|_{\mathcal{H}_{\text{qp}}^1(\Omega)} \|\mathbf{V}\|_{\mathcal{H}_{\text{qp}}^1(\Omega)}. \end{aligned}$$

Combining inequality (14) and the assumption $\tilde{F}\gamma_1^2 < \gamma_0$ yields

$$\begin{aligned} |A^{\text{PML}}(\mathbf{U}, \mathbf{V})| &\geq \gamma_0 \|\mathbf{U}\|_{\mathcal{H}_{\text{qp}}^1(\Omega)} \|\mathbf{V}\|_{\mathcal{H}_{\text{qp}}^1(\Omega)} - \tilde{F}\gamma_1^2 \|\mathbf{U}\|_{\mathcal{H}_{\text{qp}}^1(\Omega)} \|\mathbf{V}\|_{\mathcal{H}_{\text{qp}}^1(\Omega)} \\ &= (\gamma_0 - \tilde{F}\gamma_1^2) \|\mathbf{U}\|_{\mathcal{H}_{\text{qp}}^1(\Omega)} \|\mathbf{V}\|_{\mathcal{H}_{\text{qp}}^1(\Omega)}. \end{aligned}$$

Next, we turn to estimate (34). By utilizing (11), (30), Lemma 2 and Lemma 3, one can get

$$\begin{aligned} A(\mathbf{U} - \mathbf{U}^{\text{PML}}, \mathbf{V}) &= A(\mathbf{U}, \mathbf{V}) - A(\mathbf{U}^{\text{PML}}, \mathbf{V}) \\ &= A(\mathbf{U}, \mathbf{V}) - A^{\text{PML}}(\mathbf{U}^{\text{PML}}, \mathbf{V}) + A^{\text{PML}}(\mathbf{U}^{\text{PML}}, \mathbf{V}) - A(\mathbf{U}^{\text{PML}}, \mathbf{V}) \\ &= \langle (\mathcal{T}_+ - \mathcal{T}_+^{\text{PML}}) p^{\text{sc,PML}}, \varphi \rangle_{\Gamma_+} + \langle (\mathcal{T}_- - \mathcal{T}_-^{\text{PML}}) \mathbf{u}^{\text{PML}}, \psi \rangle_{\Gamma_-} \\ &\leq F_1 \|p^{\text{sc,PML}}\|_{L^2(\Gamma_+)} \|\varphi\|_{L^2(\Gamma_+)} + F_2 \|\mathbf{u}^{\text{PML}}\|_{L^2(\Gamma_-)^2} \|\psi\|_{L^2(\Gamma_-)^2} \\ &\leq F_1 \gamma_1 \|p^{\text{sc,PML}}\|_{L^2(\Gamma_+)} \|\varphi\|_{H^1(\Omega_+)} + F_2 \gamma_1 \|\mathbf{u}^{\text{PML}}\|_{L^2(\Gamma_-)^2} \|\psi\|_{H^1(\Omega_-)^2} \\ &\leq (F_1 \gamma_1 \|p^{\text{sc,PML}}\|_{L^2(\Gamma_+)} + F_2 \gamma_1 \|\mathbf{u}^{\text{PML}}\|_{L^2(\Gamma_-)^2}) \|\mathbf{V}\|_{\mathcal{H}_{\text{qp}}^1(\Omega)}, \end{aligned}$$

which completes the proof. \square

It follows from Theorem 1 that the PML approximation error can be significantly reduced by increasing the PML parameters σ_j or δ_j .

4. Discrete Problem

This section focuses on the FE discretization of the PML variational problem (17) and investigating the corresponding residual a posteriori error estimate.

4.1. FEM approximation

Let $\mathcal{M}_h = \mathcal{M}_{h,+} \cup \mathcal{M}_{h,-}$, where $\mathcal{M}_{h,+}$ and $\mathcal{M}_{h,-}$ are regular triangulations of D_+ and D_- , respectively. Assume that any triangle element T must be entirely contained within the domain $\overline{\Omega_m^{\text{PML}}}$ ($m = +, -$) or $\overline{\Omega}$. Let $\mathcal{S}_h^+ \subset H_{\text{qp}}^1(D_+)$ and $\mathcal{S}_h^- \subset H_{\text{qp}}^1(D_-)^2$ be the conforming finite element spaces, i.e.,

$$\begin{aligned} \mathcal{S}_h^+ &:= \left\{ p_h \in C(\overline{\Omega}_+): p_h|_T \in P_k(T), \forall T \in \mathcal{M}_{h,+}, p_h(\Lambda, x_2) = p_h(0, x_2) e^{i\alpha\Lambda} \right\}, \\ \mathcal{S}_h^- &:= \left\{ \mathbf{u}_h \in C(\overline{\Omega}_-): \mathbf{u}_h|_T \in P_k(T)^2, \forall T \in \mathcal{M}_{h,-}, \mathbf{u}_h(\Lambda, x_2) = \mathbf{u}_h(0, x_2) e^{i\alpha\Lambda} \right\}, \end{aligned}$$

where $P_k(T)$ denotes the set of all polynomials of degree no more than k ($k \in \mathbb{N}^+$). Let $\mathcal{H}_h^1(D) := \mathcal{S}_h^+ \times \mathcal{S}_h^- \subset \mathcal{H}^1(D)$ and $\overset{\circ}{\mathcal{H}}_h(D) = \mathcal{H}_h^1(D) \cap \mathcal{H}_{0,\text{qp}}^1(D)$. The FE approximation to (17) is formulated as: Given p^{in} , seek $\hat{\mathbf{U}}_h \in \mathcal{H}_h^1(D)$ such that $\hat{p}_h^{\text{sc}} = 0$ on Γ_+^{PML} , $\hat{\mathbf{u}}_h = 0$ on Γ_-^{PML} , and

$$B_D(\hat{\mathbf{U}}_h, \mathbf{V}_h) = L(\mathbf{V}_h), \quad \forall \mathbf{V}_h = (\varphi_h, \psi_h) \in \overset{\circ}{\mathcal{H}}_h(D). \quad (35)$$

where $B_D(\cdot, \cdot)$ is a sesquilinear form defined by (18).

This paper aims to develop a residual-based a posteriori error estimate as well as the adaptive FE algorithm. Therefore, we assume that the variational problem (35) is uniquely solvable.

4.2. Error representation

In this subsection, we mainly introduce an error representation formula, which is used to facilitate the a posteriori error analysis in Theorem 2. For any $\mathbf{V} = (\varphi, \psi) \in \mathcal{H}_{qp}^1(\Omega)$, let $\tilde{\mathbf{V}}$ be the extension of \mathbf{V} such that $\tilde{\mathbf{V}} = \mathbf{V}$ in Ω and $\tilde{\mathbf{V}}$ satisfies the following boundary value problem

$$\begin{aligned} \Delta_{\hat{x}} \tilde{\varphi} + \kappa^2 \tilde{\varphi} &= 0 & \text{in } \Omega_+^{\text{PML}}, \\ \Delta_{\hat{x}}^* \tilde{\psi} + \omega^2 \rho \tilde{\psi} &= 0 & \text{in } \Omega_-^{\text{PML}}, \\ \tilde{\varphi}(x_1, h_1) &= \varphi(x_1, h_1) & \text{on } \Gamma_+, \\ \tilde{\psi}(x_1, h_2) &= \psi(x_1, h_2) & \text{on } \Gamma_-, \\ \tilde{\varphi}(x_1, h_1 + \delta_1) &= 0 & \text{on } \Gamma_+^{\text{PML}}, \\ \tilde{\psi}(x_1, h_2 - \delta_2) &= 0 & \text{on } \Gamma_-^{\text{PML}}. \end{aligned} \tag{36}$$

We give the following two lemmas, which will be used in the subsequent a posteriori estimate.

Lemma 4. For any $(p, \mathbf{u}) \in \mathcal{H}_{qp}^1(\Omega)$, $(\varphi, \psi) \in \mathcal{H}_{qp}^1(\Omega)$, one can obtain

$$\begin{aligned} \int_{\Gamma_+} \mathcal{T}_+^{\text{PML}} p \bar{\varphi} \, ds &= \int_{\Gamma_+} p \partial_{x_2} \bar{\varphi} \, ds, \\ \int_{\Gamma_-} \mathcal{T}_-^{\text{PML}} \mathbf{u} \cdot \bar{\psi} \, ds &= \int_{\Gamma_-} \mathbf{u} \cdot \mathcal{B} \bar{\psi} \, ds. \end{aligned}$$

Proof. To begin with, we introduce $\hat{z} \in H_{qp}^1(\Omega_+^{\text{PML}})$ and $\hat{\mathbf{w}} \in H_{qp}^1(\Omega_-^{\text{PML}})$ satisfying

$$\begin{aligned} \Delta_{\hat{x}} \hat{z} + \kappa^2 \hat{z} &= 0 & \text{in } \Omega_+^{\text{PML}}, \\ \Delta_{\hat{x}}^* \hat{\mathbf{w}} + \omega^2 \rho \hat{\mathbf{w}} &= 0 & \text{in } \Omega_-^{\text{PML}}, \\ \hat{z}(x_1, h_1) &= p(x_1, h_1) & \text{on } \Gamma_+, \\ \hat{\mathbf{w}}(x_1, h_2) &= \mathbf{u}(x_1, h_2) & \text{on } \Gamma_-, \\ \hat{z}(x_1, h_1 + \delta_1) &= 0 & \text{on } \Gamma_+^{\text{PML}}, \\ \hat{\mathbf{w}}(x_1, h_2 - \delta_2) &= 0 & \text{on } \Gamma_-^{\text{PML}}. \end{aligned}$$

It follows from the definitions of $\mathcal{T}_+^{\text{PML}}$ and $\mathcal{T}_-^{\text{PML}}$ that

$$\begin{aligned} \mathcal{T}_+^{\text{PML}} p &= \partial_{x_2} \hat{z} & \text{on } \Gamma_+, \\ \mathcal{T}_-^{\text{PML}} \mathbf{u} &= \mathcal{B} \hat{\mathbf{w}} & \text{on } \Gamma_-. \end{aligned}$$

By combining Green's formula and the extension, we have

$$\begin{aligned} \int_{\Gamma_+} p \partial_{x_2} \bar{\varphi} \, ds &= \int_{\Gamma_+} \hat{z} \partial_{x_2} \bar{\varphi} \, ds = - \int_{\Omega_+^{\text{PML}}} [\nabla_{\hat{x}} \bar{\varphi} \cdot \nabla_{\hat{x}} \hat{z} - \kappa^2 \bar{\varphi} \hat{z}] \, d\mathbf{x} \\ &= \int_{\Omega_+^{\text{PML}}} (\Delta_{\hat{x}} \hat{z} + \kappa^2 \hat{z}) \bar{\varphi} \, d\mathbf{x} + \int_{\Gamma_+} \partial_{x_2} \hat{z} \bar{\varphi} \, ds \\ &= \int_{\Gamma_+} \partial_{x_2} \hat{z} \bar{\varphi} \, ds = \int_{\Gamma_+} \mathcal{T}_+^{\text{PML}} p \bar{\varphi} \, ds. \end{aligned}$$

Similarly, using the first Betti's formula and the extension yields

$$\begin{aligned}
\int_{\Gamma_-} \mathbf{u} \cdot \mathcal{B} \bar{\psi} \, ds &= \int_{\Gamma_-} \hat{\mathbf{w}} \cdot \mathcal{B} \bar{\psi} \, ds \\
&= - \int_{\Omega_-^{\text{PML}}} \left[\lambda (\nabla_{\hat{\mathbf{x}}} \cdot \bar{\psi}) (\nabla_{\hat{\mathbf{x}}} \cdot \hat{\mathbf{w}}) + \frac{\mu}{2} \left(\nabla_{\hat{\mathbf{x}}} \bar{\psi} + \nabla_{\hat{\mathbf{x}}} \bar{\psi}^\top \right) : \left(\nabla_{\hat{\mathbf{x}}} \hat{\mathbf{w}} + \nabla_{\hat{\mathbf{x}}} \hat{\mathbf{w}}^\top \right) - \omega^2 \rho \bar{\psi} \cdot \hat{\mathbf{w}} \right] \, dx \\
&= \int_{\Omega_-^{\text{PML}}} \left(\Delta_{\hat{\mathbf{x}}}^* \hat{\mathbf{w}} + \omega^2 \rho \hat{\mathbf{w}} \right) \cdot \bar{\psi} \, dx + \int_{\Gamma_-} \mathcal{B} \hat{\mathbf{w}} \cdot \bar{\psi} \, ds \\
&= \int_{\Gamma_-} \mathcal{B} \hat{\mathbf{w}} \cdot \bar{\psi} \, ds = \int_{\Gamma_-} \mathcal{T}_-^{\text{PML}} \mathbf{u} \cdot \bar{\psi} \, ds,
\end{aligned}$$

which completes the proof. \square

Lemma 5. For any $\mathbf{V} = (\varphi, \psi) \in \mathcal{H}_{\text{qp}}^1(\Omega)$, let $\tilde{\mathbf{V}} \in \mathcal{H}_{0,\text{qp}}^1(\mathbf{D})$ be the extension of \mathbf{V} which satisfies (36). Then there holds

$$\begin{aligned}
\|\nabla \tilde{\varphi}\|_{L^2(\Omega_+^{\text{PML}})} &\leq \gamma_1 C_1 \|\varphi\|_{H^1(\Omega_+)}, \\
\|\nabla \tilde{\psi}\|_{F(\Omega_-^{\text{PML}})} &\leq \gamma_1 C_2 \|\psi\|_{H^1(\Omega_-)^2},
\end{aligned}$$

where $C_1 > 0$ and $C_2 > 0$ are constants, and the Frobenius norm of the Jacobian matrix $\nabla \psi$ is defined by

$$\|\nabla \psi\|_{F(R)} = \left(\sum_{j=1}^2 \int_R |\nabla \psi_j|^2 \, dx \right)^{1/2}, \quad \text{for any subdomain } R \subset \mathbb{R}^2.$$

Proof. The proof follows a methodology analogous to that employed in [16, Lemma 4.3] and [30, Lemma 4.3]. For brevity, the corresponding detailed derivations are omitted. \square

For notational simplicity, we write $\tilde{\mathbf{V}}$ as \mathbf{V} in the sequel, unless stated otherwise. The following lemma gives an error representation formula, which plays a key role in the analysis of the a posteriori estimate.

Lemma 6. For any $\mathbf{V} = (\varphi, \psi) \in \mathcal{H}_{\text{qp}}^1(\Omega)$, which can be extended to be a function in $\mathcal{H}_{0,\text{qp}}^1(\mathbf{D})$. Based on (36), and $\mathbf{V}_h = (\varphi_h, \psi_h) \in \mathcal{H}_h^{\circ}(\mathbf{D})$, there holds

$$\begin{aligned}
A(\mathbf{U} - \hat{\mathbf{U}}_h, \mathbf{V}) &= L(\mathbf{V} - \mathbf{V}_h) - B_{\mathbf{D}}(\hat{\mathbf{U}}_h, \mathbf{V} - \mathbf{V}_h) \\
&\quad + \int_{\Gamma_+} (\mathcal{T}_+ - \mathcal{T}_+^{\text{PML}}) \hat{p}_h^{\text{sc}} \bar{\varphi} \, ds + \int_{\Gamma_-} (\mathcal{T}_- - \mathcal{T}_-^{\text{PML}}) \hat{\mathbf{u}}_h \cdot \bar{\psi} \, ds.
\end{aligned} \tag{37}$$

Proof. By (11), (12), (30) and (31), one can get

$$\begin{aligned}
A(\mathbf{U} - \hat{\mathbf{U}}_h, \mathbf{V}) &= A(\mathbf{U} - \hat{\mathbf{U}}, \mathbf{V}) + A(\hat{\mathbf{U}} - \hat{\mathbf{U}}_h, \mathbf{V}) \\
&= A(\mathbf{U} - \hat{\mathbf{U}}, \mathbf{V}) + A(\hat{\mathbf{U}} - \hat{\mathbf{U}}_h, \mathbf{V}) - A^{\text{PML}}(\hat{\mathbf{U}} - \hat{\mathbf{U}}_h, \mathbf{V}) + A^{\text{PML}}(\hat{\mathbf{U}} - \hat{\mathbf{U}}_h, \mathbf{V}) \\
&= A(\mathbf{U}, \mathbf{V}) - A(\hat{\mathbf{U}}, \mathbf{V}) + A^{\text{PML}}(\hat{\mathbf{U}} - \hat{\mathbf{U}}_h, \mathbf{V}) \\
&\quad - \int_{\Gamma_+} (\mathcal{T}_+ - \mathcal{T}_+^{\text{PML}})(\hat{p}^{\text{sc}} - \hat{p}_h^{\text{sc}}) \bar{\varphi} \, ds - \int_{\Gamma_-} (\mathcal{T}_- - \mathcal{T}_-^{\text{PML}})(\hat{\mathbf{u}} - \hat{\mathbf{u}}_h) \cdot \bar{\psi} \, ds \\
&= A(\mathbf{U}, \mathbf{V}) - A(\hat{\mathbf{U}}, \mathbf{V}) + A^{\text{PML}}(\hat{\mathbf{U}}, \mathbf{V}) - A^{\text{PML}}(\hat{\mathbf{U}}, \mathbf{V}) + A^{\text{PML}}(\hat{\mathbf{U}} - \hat{\mathbf{U}}_h, \mathbf{V}) \\
&\quad - \int_{\Gamma_+} (\mathcal{T}_+ - \mathcal{T}_+^{\text{PML}})(\hat{p}^{\text{sc}} - \hat{p}_h^{\text{sc}}) \bar{\varphi} \, ds - \int_{\Gamma_-} (\mathcal{T}_- - \mathcal{T}_-^{\text{PML}})(\hat{\mathbf{u}} - \hat{\mathbf{u}}_h) \cdot \bar{\psi} \, ds \\
&= \int_{\Gamma_+} (\mathcal{T}_+ - \mathcal{T}_+^{\text{PML}}) \hat{p}^{\text{sc}} \bar{\varphi} \, ds + \int_{\Gamma_-} (\mathcal{T}_- - \mathcal{T}_-^{\text{PML}}) \hat{\mathbf{u}} \cdot \bar{\psi} \, ds + A^{\text{PML}}(\hat{\mathbf{U}} - \hat{\mathbf{U}}_h, \mathbf{V}) \\
&\quad - \int_{\Gamma_+} (\mathcal{T}_+ - \mathcal{T}_+^{\text{PML}})(\hat{p}^{\text{sc}} - \hat{p}_h^{\text{sc}}) \bar{\varphi} \, ds - \int_{\Gamma_-} (\mathcal{T}_- - \mathcal{T}_-^{\text{PML}})(\hat{\mathbf{u}} - \hat{\mathbf{u}}_h) \cdot \bar{\psi} \, ds \\
&= \int_{\Gamma_+} (\mathcal{T}_+ - \mathcal{T}_+^{\text{PML}}) \hat{p}_h^{\text{sc}} \bar{\varphi} \, ds + \int_{\Gamma_-} (\mathcal{T}_- - \mathcal{T}_-^{\text{PML}}) \hat{\mathbf{u}}_h \cdot \bar{\psi} \, ds + A^{\text{PML}}(\hat{\mathbf{U}} - \hat{\mathbf{U}}_h, \mathbf{V}). \tag{38}
\end{aligned}$$

Combining equation (31) and Lemma 4 yields

$$\begin{aligned}
A^{\text{PML}}(\hat{\mathbf{U}} - \hat{\mathbf{U}}_h, \mathbf{V}) &= B_\Omega(\hat{\mathbf{U}} - \hat{\mathbf{U}}_h, \mathbf{V}) - \int_{\Gamma_+} \mathcal{T}_+^{\text{PML}}(\hat{p}^{\text{sc}} - \hat{p}_h^{\text{sc}}) \bar{\varphi} \, ds - \int_{\Gamma_-} \mathcal{T}_-^{\text{PML}}(\hat{\mathbf{u}} - \hat{\mathbf{u}}_h) \cdot \bar{\psi} \, ds \\
&= B_\Omega(\hat{\mathbf{U}} - \hat{\mathbf{U}}_h, \mathbf{V}) - \int_{\Gamma_+} (\hat{p}^{\text{sc}} - \hat{p}_h^{\text{sc}}) \partial_{x_2} \bar{\varphi} \, ds - \int_{\Gamma_-} (\hat{\mathbf{u}} - \hat{\mathbf{u}}_h) \cdot \mathcal{B} \bar{\psi} \, ds.
\end{aligned}$$

Due to $\mathcal{L}_1 \bar{\varphi} = 0$ in Ω_+^{PML} and $\mathcal{L}_2 \bar{\psi} = 0$ in Ω_-^{PML} , it follows from the Green's formula and the first Betti's formula that

$$\begin{aligned}
0 &= - \int_{\Omega_+^{\text{PML}}} \mathcal{L}_1 \bar{\varphi} (\hat{p}^{\text{sc}} - \hat{p}_h^{\text{sc}}) \, d\mathbf{x} \\
&= \int_{\Omega_+^{\text{PML}}} [\mathbb{A} \nabla \bar{\varphi} \cdot \nabla (\hat{p}^{\text{sc}} - \hat{p}_h^{\text{sc}}) - \kappa^2 s(x_2) \bar{\varphi} (\hat{p}^{\text{sc}} - \hat{p}_h^{\text{sc}})] \, d\mathbf{x} - \int_{\Gamma_+^{\text{PML}}} (\hat{p}^{\text{sc}} - \hat{p}_h^{\text{sc}}) \partial_{x_2} \bar{\varphi} \, ds + \int_{\Gamma_+} (\hat{p}^{\text{sc}} - \hat{p}_h^{\text{sc}}) \partial_{x_2} \bar{\varphi} \, ds
\end{aligned}$$

and

$$\begin{aligned}
0 &= - \int_{\Omega_-^{\text{PML}}} \mathcal{L}_2 \bar{\psi} \cdot (\hat{\mathbf{u}} - \hat{\mathbf{u}}_h) \, d\mathbf{x} \\
&= \int_{\Omega_-^{\text{PML}}} [\mathcal{S}_{\lambda, \mu}(\hat{\mathbf{u}} - \hat{\mathbf{u}}_h, \psi) - \omega^2 s(x_2) \rho (\hat{\mathbf{u}} - \hat{\mathbf{u}}_h) \cdot \bar{\psi}] \, d\mathbf{x} - \int_{\Gamma_-^{\text{PML}}} (\hat{\mathbf{u}} - \hat{\mathbf{u}}_h) \cdot \mathcal{B} \bar{\psi} \, ds + \int_{\Gamma_-} (\hat{\mathbf{u}} - \hat{\mathbf{u}}_h) \cdot \mathcal{B} \bar{\psi} \, ds.
\end{aligned}$$

Furthermore, it follows from (17), (35) and the above two equalities that

$$\begin{aligned}
A^{\text{PML}}(\hat{\mathbf{U}} - \hat{\mathbf{U}}_h, \mathbf{V}) &= B_{\Omega}(\hat{\mathbf{U}} - \hat{\mathbf{U}}_h, \mathbf{V}) - \int_{\Gamma_+} (\hat{p}^{\text{sc}} - \hat{p}_h^{\text{sc}}) \partial_{x_2} \bar{\varphi} \, ds - \int_{\Gamma_-} (\hat{\mathbf{u}} - \hat{\mathbf{u}}_h) \cdot \mathcal{B} \bar{\psi} \, ds \\
&= B_{\text{D}}(\hat{\mathbf{U}} - \hat{\mathbf{U}}_h, \mathbf{V}) - \int_{\Gamma_+^{\text{PML}}} (\hat{p}^{\text{sc}} - \hat{p}_h^{\text{sc}}) \partial_{\hat{x}_2} \bar{\varphi} \, ds - \int_{\Gamma_-^{\text{PML}}} (\hat{\mathbf{u}} - \hat{\mathbf{u}}_h) \cdot \mathcal{B}_{\hat{x}} \bar{\psi} \, ds \\
&= B_{\text{D}}(\hat{\mathbf{U}}, \mathbf{V}) - B_{\text{D}}(\hat{\mathbf{U}}_h, \mathbf{V}) + B_{\text{D}}(\hat{\mathbf{U}}_h, \mathbf{V}_h) - B_{\text{D}}(\hat{\mathbf{U}}_h, \mathbf{V}_h) \\
&\quad - \int_{\Gamma_+^{\text{PML}}} (\hat{p}^{\text{sc}} - \hat{p}_h^{\text{sc}}) \partial_{\hat{x}_2} \bar{\varphi} \, ds - \int_{\Gamma_-^{\text{PML}}} (\hat{\mathbf{u}} - \hat{\mathbf{u}}_h) \cdot \mathcal{B}_{\hat{x}} \bar{\psi} \, ds \\
&= L(\mathbf{V}) - B_{\text{D}}(\hat{\mathbf{U}}_h, \mathbf{V} - \mathbf{V}_h) - L(\mathbf{V}_h) \\
&\quad - \int_{\Gamma_+^{\text{PML}}} (\hat{p}^{\text{sc}} - \hat{p}_h^{\text{sc}}) \partial_{\hat{x}_2} \bar{\varphi} \, ds - \int_{\Gamma_-^{\text{PML}}} (\hat{\mathbf{u}} - \hat{\mathbf{u}}_h) \cdot \mathcal{B}_{\hat{x}} \bar{\psi} \, ds \\
&= L(\mathbf{V} - \mathbf{V}_h) - B_{\text{D}}(\hat{\mathbf{U}}_h, \mathbf{V} - \mathbf{V}_h) - \int_{\Gamma_+^{\text{PML}}} (\hat{p}^{\text{sc}} - \hat{p}_h^{\text{sc}}) \partial_{\hat{x}_2} \bar{\varphi} \, ds - \int_{\Gamma_-^{\text{PML}}} (\hat{\mathbf{u}} - \hat{\mathbf{u}}_h) \cdot \mathcal{B}_{\hat{x}} \bar{\psi} \, ds. \quad (39)
\end{aligned}$$

Substituting (39) into (38) gives

$$\begin{aligned}
A(\mathbf{U} - \hat{\mathbf{U}}_h, \mathbf{V}) &= L(\mathbf{V} - \mathbf{V}_h) - B_{\text{D}}(\hat{\mathbf{U}}_h, \mathbf{V} - \mathbf{V}_h) \\
&\quad + \int_{\Gamma_+} (\mathcal{T}_+ - \mathcal{T}_+^{\text{PML}}) \hat{p}_h^{\text{sc}} \bar{\varphi} \, ds + \int_{\Gamma_-} (\mathcal{T}_s - \mathcal{T}_s^{\text{PML}}) \hat{\mathbf{u}}_h \cdot \bar{\psi} \, ds,
\end{aligned}$$

where we have used $\hat{p}^{\text{sc}} = \hat{p}_h^{\text{sc}} = 0$ on Γ_+^{PML} and $\hat{\mathbf{u}} = \hat{\mathbf{u}}_h = 0$ on Γ_-^{PML} . Thus the proof is completed. \square

4.3. A posteriori error analysis

In this subsection, we introduce the definition of a posteriori error indicators. For any $T \in \mathcal{M}_h$, define h_T as its diameter. Let ∂T be the set of all the edges of T that do not lie on Γ_+^{PML} and Γ_-^{PML} . For any $e \in \partial T$, define h_e as its length. Let

$$\begin{aligned}
\mathcal{R}_+ \hat{p}_h^{\text{sc}} &:= \mathcal{L}_1 \hat{p}_h^{\text{sc}}, \quad \forall T \in \mathcal{M}_{h,+}, \\
\mathcal{R}_- \hat{\mathbf{u}}_h &:= \mathcal{L}_2 \hat{\mathbf{u}}_h, \quad \forall T \in \mathcal{M}_{h,-}.
\end{aligned}$$

For any $T_1^+, T_2^+ \in \mathcal{M}_{h,+}$, the jump residual $J_{e,+}$ is given by

$$J_{e,+} := \begin{cases} -(\mathbb{A} \nabla \hat{p}_h^{\text{sc}}|_{T_1^+} \cdot \mathbf{v}_1 + \mathbb{A} \nabla \hat{p}_h^{\text{sc}}|_{T_2^+} \cdot \mathbf{v}_2), & e \in \partial T_1^+ \cap \partial T_2^+, \\ 2(\partial_{\mathbf{n}}(p^{\text{in}} + \hat{p}_h^{\text{sc}}) - \rho_f \omega^2 \hat{\mathbf{u}}_h \cdot \mathbf{n}), & e \in \Gamma. \end{cases}$$

where \mathbf{v}_j is the unit outward normal vector on the boundary of T_j^+ ($j = 1, 2$). For any $T_1^-, T_2^- \in \mathcal{M}_{h,-}$, the jump residual $J_{e,-}$ is given by

$$J_{e,-} := \begin{cases} -(\mathbf{T} \hat{\mathbf{u}}_h|_{T_1^-} + \mathbf{T} \hat{\mathbf{u}}_h|_{T_2^-}), & e \in \partial T_1^- \cap \partial T_2^-, \\ -2((p^{\text{in}} + \hat{p}_h^{\text{sc}}) \mathbf{n} + \mathbf{T} \hat{\mathbf{u}}_h), & e \in \Gamma. \end{cases}$$

Next we consider the jump residual on the left line segment Γ_{left} and right line segment Γ_{right} , where

$$\begin{aligned}
\Gamma_{\text{left}} &= \{(x_1, x_2) : x_1 = 0, h_2 - \delta_2 < x_2 < h_1 + \delta_1\}, \\
\Gamma_{\text{right}} &= \{(x_1, x_2) : x_1 = \Lambda, h_2 - \delta_2 < x_2 < h_1 + \delta_1\}.
\end{aligned}$$

For any $e \in \Gamma_{\text{left}} \cap \partial T_1$ for some $T_1 \in \mathcal{M}_h$ and its corresponding edge $e' \in \Gamma_{\text{right}} \cap \partial T_2$ for some $T_2 \in \mathcal{M}_h$, denote the jump residual by

$$\begin{aligned}
J_{e,+} &:= -(\mathbb{A} \nabla \hat{p}_h^{\text{sc}}|_{T_1} \cdot \mathbf{v}_1 + e^{-i\alpha\Lambda} \mathbb{A} \nabla \hat{p}_h^{\text{sc}}|_{T_2} \cdot \mathbf{v}_2), \\
J_{e',+} &:= -(e^{i\alpha\Lambda} \mathbb{A} \nabla \hat{p}_h^{\text{sc}}|_{T_1} \cdot \mathbf{v}_1 + \mathbb{A} \nabla \hat{p}_h^{\text{sc}}|_{T_2} \cdot \mathbf{v}_2),
\end{aligned}$$

and

$$\begin{aligned}\mathbf{J}_{e,-} &:= -\left(\mathbf{T}\hat{\mathbf{u}}_h|_{T_1} + e^{-i\alpha\Lambda}\mathbf{T}\hat{\mathbf{u}}_h|_{T_2}\right), \\ \mathbf{J}_{e',-} &:= -\left(e^{i\alpha\Lambda}\mathbf{T}\hat{\mathbf{u}}_h|_{T_1} + \mathbf{T}\hat{\mathbf{u}}_h|_{T_2}\right).\end{aligned}$$

For $T \in \mathcal{M}_{h,+}$ and $T \in \mathcal{M}_{h,-}$, denote the local error estimators by $\eta_{T,+}$ and $\eta_{T,-}$, where

$$\eta_{T,+} = h_T \|\mathcal{R}_+ \hat{p}_h^{\text{sc}}\|_{L^2(T)} + \left(\frac{1}{2} \sum_{e \in \partial T} h_e \|\mathbf{J}_{e,+}\|_{L^2(e)}^2\right)^{1/2}, \quad (40)$$

$$\eta_{T,-} = h_T \|\mathcal{R}_- \hat{\mathbf{u}}_h\|_{L^2(T)^2} + \left(\frac{1}{2} \sum_{e \in \partial T} h_e \|\mathbf{J}_{e,-}\|_{L^2(e)^2}^2\right)^{1/2}. \quad (41)$$

Now we are ready to give the main result.

Theorem 2. *There exists a positive constant C such that the following a posteriori error estimate holds*

$$\begin{aligned}\|\mathbf{U} - \hat{\mathbf{U}}_h\|_{\mathcal{H}_{\text{qp}}^1(\Omega)} &\leq \max\{C(1 + \gamma_1 C_1), C(1 + \gamma_1 C_2)\} \left(\sum_{T \in \mathcal{M}_{h,+}} \eta_{T,+}^2 + \sum_{T \in \mathcal{M}_{h,-}} \eta_{T,-}^2 \right)^{1/2} \\ &\quad + \gamma_1 F_1 \|\hat{p}_h^{\text{sc}}\|_{L^2(\Gamma_+)} + \gamma_1 F_2 \|\hat{\mathbf{u}}_h\|_{L^2(\Gamma_-)^2},\end{aligned}$$

where γ_1 , F_j and C_j ($j = 1, 2$) are constants defined in Lemmas 2, 3 and 5, respectively.

Proof. For brevity, we can rewrite the formula (37) as

$$A(\mathbf{U} - \hat{\mathbf{U}}_h, \mathbf{V}) = J_1 + J_2, \quad (42)$$

where

$$\begin{aligned}J_1 &= L(\mathbf{V} - \mathbf{V}_h) - B_D(\hat{\mathbf{U}}_h, \mathbf{V} - \mathbf{V}_h), \\ J_2 &= \int_{\Gamma_+} (\mathcal{T}_+ - \mathcal{T}_+^{\text{PML}}) \hat{p}_h^{\text{sc}} \bar{\varphi} \, ds + \int_{\Gamma_-} (\mathcal{T}_- - \mathcal{T}_-^{\text{PML}}) \hat{\mathbf{u}}_h \cdot \bar{\boldsymbol{\psi}} \, ds.\end{aligned}$$

Take $\varphi_h = \Pi_h^+ \varphi \in H_{0,\text{qp}}^1(\mathbf{D}_+)$ and $\boldsymbol{\psi}_h = \Pi_h^- \boldsymbol{\psi} \in H_{0,\text{qp}}^1(\mathbf{D}_-)^2$, where Π_h^+ and Π_h^- are Scott-Zhang interpolation operators (cf. [46]) satisfying the following estimates

$$\|\varphi - \Pi_h^+ \varphi\|_{L^2(T)} \leq Ch_T \|\nabla \varphi\|_{L^2(\tilde{T})}, \quad \|\varphi - \Pi_h^+ \varphi\|_{L^2(e)} \leq Ch_e^{1/2} \|\nabla \varphi\|_{L^2(\tilde{e})}, \quad (43)$$

$$\|\boldsymbol{\psi} - \Pi_h^- \boldsymbol{\psi}\|_{L^2(T)^2} \leq Ch_T \|\nabla \boldsymbol{\psi}\|_{F(\tilde{T})}, \quad \|\boldsymbol{\psi} - \Pi_h^- \boldsymbol{\psi}\|_{L^2(e)^2} \leq Ch_e^{1/2} \|\nabla \boldsymbol{\psi}\|_{F(\tilde{e})}. \quad (44)$$

Here, \tilde{T} and \tilde{e} are the union of all elements in $\mathcal{M}_{h,+} \cup \mathcal{M}_{h,-}$, which have nonempty intersection with T and e , respectively. By the definition of $B_D(\cdot, \cdot)$ and $L(\cdot)$ in (35), one has

$$\begin{aligned}J_1 &= \sum_{T \in \mathcal{M}_{h,+}} \left(\int_T \left(-\mathbb{A} \nabla \hat{p}_h^{\text{sc}} \cdot \nabla (\bar{\varphi} - \Pi_h^+ \bar{\varphi}) + \kappa^2 s(x_2) \hat{p}_h^{\text{sc}} (\bar{\varphi} - \Pi_h^+ \bar{\varphi}) \right) \, dx \right. \\ &\quad \left. + \sum_{e \in \partial T \cap \Gamma} \int_e (\partial_{\mathbf{n}} p^{\text{in}} - \rho_f \omega^2 \hat{\mathbf{u}}_h \cdot \mathbf{n}) (\bar{\varphi} - \Pi_h^+ \bar{\varphi}) \, ds \right) \\ &\quad + \sum_{T \in \mathcal{M}_{h,-}} \left(\int_T -\mathcal{S}_{\lambda,\mu} (\hat{\mathbf{u}}_h, \boldsymbol{\psi} - \Pi_h^- \boldsymbol{\psi}) + \omega^2 s(x_2) \rho \hat{\mathbf{u}}_h \cdot (\bar{\boldsymbol{\psi}} - \Pi_h^- \bar{\boldsymbol{\psi}}) \, dx \right. \\ &\quad \left. + \sum_{e \in \partial T \cap \Gamma} \int_e - (p^{\text{in}} + \hat{p}_h^{\text{sc}}) \mathbf{n} \cdot (\bar{\boldsymbol{\psi}} - \Pi_h^- \bar{\boldsymbol{\psi}}) \, ds \right).\end{aligned}$$

Applying the integration by parts yields

$$\begin{aligned}
J_1 &= \sum_{T \in \mathcal{M}_{h,+}} \left(\int_T \mathcal{L}_1 \hat{p}_h^{\text{sc}} (\bar{\varphi} - \Pi_h^+ \bar{\varphi}) \, dx - \sum_{e \in \partial T} \int_e \mathbb{A} \nabla \hat{p}_h^{\text{sc}} \cdot \nu (\bar{\varphi} - \Pi_h^+ \bar{\varphi}) \, ds \right. \\
&\quad \left. + \sum_{e \in \partial T \cap \Gamma} \int_e (\partial_n p^{\text{in}} - \rho_f \omega^2 \hat{\mathbf{u}}_h \cdot \mathbf{n}) (\bar{\varphi} - \Pi_h^+ \bar{\varphi}) \, ds \right) \\
&\quad + \sum_{T \in \mathcal{M}_{h,-}} \left(\int_T \mathcal{L}_2 \hat{\mathbf{u}}_h \cdot (\bar{\psi} - \Pi_h^- \bar{\psi}) \, dx - \sum_{e \in \partial T} \int_e \mathbf{T} \hat{\mathbf{u}}_h (\bar{\psi} - \Pi_h^- \bar{\psi}) \, dx \right. \\
&\quad \left. + \sum_{e \in \partial T \cap \Gamma} \int_e (p^{\text{in}} + \hat{p}_h^{\text{sc}}) \mathbf{n} \cdot (\bar{\psi} - \Pi_h^- \bar{\psi}) \, ds \right) \\
&= \sum_{T \in \mathcal{M}_{h,+}} \left(\int_T \mathcal{R}_+ \hat{p}_h^{\text{sc}} (\bar{\varphi} - \Pi_h^+ \bar{\varphi}) \, dx + \sum_{e \in \partial T} \frac{1}{2} \int_e J_{e,+} (\bar{\varphi} - \Pi_h^+ \bar{\varphi}) \, ds \right) \\
&\quad + \sum_{T \in \mathcal{M}_{h,-}} \left(\int_T \mathcal{R}_- \hat{\mathbf{u}}_h \cdot (\bar{\psi} - \Pi_h^- \bar{\psi}) \, dx + \sum_{e \in \partial T} \frac{1}{2} \int_e \mathbf{J}_{e,-} \cdot (\bar{\psi} - \Pi_h^- \bar{\psi}) \, ds \right).
\end{aligned}$$

It follows from (43) and (44) that

$$\begin{aligned}
|J_1| &\leq \sum_{T \in \mathcal{M}_{h,+}} \left(Ch_T \|\mathcal{R}_+ \hat{p}_h^{\text{sc}}\|_{L^2(T)} \|\nabla \varphi\|_{L^2(\tilde{T})} + \sum_{e \in \partial T} \frac{1}{2} Ch_e^{1/2} \|J_{e,+}\|_{L^2(e)} \|\nabla \varphi\|_{L^2(\tilde{e})} \right) \\
&\quad + \sum_{T \in \mathcal{M}_{h,-}} \left(Ch_T \|\mathcal{R}_- \hat{\mathbf{u}}_h\|_{L^2(T)^2} \|\nabla \psi\|_{F(\tilde{T})} + \sum_{e \in \partial T} \frac{1}{2} Ch_e^{1/2} \|\mathbf{J}_{e,-}\|_{L^2(e)^2} \|\nabla \psi\|_{F(\tilde{e})} \right) \\
&\leq C \sum_{T \in \mathcal{M}_{h,+}} \left(h_T \|\mathcal{R}_+ \hat{p}_h^{\text{sc}}\|_{L^2(T)} + \left(\frac{1}{2} \sum_{e \in \partial T} h_e \|J_{e,+}\|_{L^2(e)}^2 \right)^{1/2} \right) \|\nabla \varphi\|_{L^2(\tilde{T})} \\
&\quad + C \sum_{T \in \mathcal{M}_{h,-}} \left(h_T \|\mathcal{R}_- \hat{\mathbf{u}}_h\|_{L^2(T)^2} + \left(\frac{1}{2} \sum_{e \in \partial T} h_e \|\mathbf{J}_{e,-}\|_{L^2(e)^2}^2 \right)^{1/2} \right) \|\nabla \psi\|_{F(\tilde{T})} \\
&\leq C \sum_{T \in \mathcal{M}_{h,+}} \eta_{T,+} \|\nabla \varphi\|_{L^2(\tilde{T})} + C \sum_{T \in \mathcal{M}_{h,-}} \eta_{T,-} \|\nabla \psi\|_{F(\tilde{T})}.
\end{aligned}$$

Using Lemma 5 and the Cauchy-Schwarz inequality gives

$$\begin{aligned}
|J_1| &\leq C(1 + \gamma_1 C_1) \left(\sum_{T \in \mathcal{M}_{h,+}} \eta_{T,+}^2 \right)^{1/2} \|\varphi\|_{H^1(\Omega_+)} + C(1 + \gamma_1 C_2) \left(\sum_{T \in \mathcal{M}_{h,-}} \eta_{T,-}^2 \right)^{1/2} \|\psi\|_{H^1(\Omega_-)^2} \\
&\leq \max \{C(1 + \gamma_1 C_1), C(1 + \gamma_1 C_2)\} \left(\sum_{T \in \mathcal{M}_{h,+}} \eta_{T,+}^2 + \sum_{T \in \mathcal{M}_{h,-}} \eta_{T,-}^2 \right)^{1/2} \|V\|_{\mathcal{H}_{\text{qp}}^1(\Omega)}
\end{aligned}$$

By Lemmas 2 and 3, we have

$$\begin{aligned}
|J_2| &\leq F_1 \|\hat{p}_h^{\text{sc}}\|_{L^2(\Gamma_+)} \|\varphi\|_{L^2(\Gamma_+)} + F_2 \|\hat{\mathbf{u}}_h\|_{L^2(\Gamma_-)^2} \|\psi\|_{L^2(\Gamma_-)^2} \\
&\leq \gamma_1 F_1 \|\hat{p}_h^{\text{sc}}\|_{L^2(\Gamma_+)} \|\varphi\|_{H^1(\Omega_+)} + \gamma_1 F_2 \|\hat{\mathbf{u}}_h\|_{L^2(\Gamma_-)^2} \|\psi\|_{H^1(\Omega_-)^2} \\
&\leq (\gamma_1 F_1 \|\hat{p}_h^{\text{sc}}\|_{L^2(\Gamma_+)} + \gamma_1 F_2 \|\hat{\mathbf{u}}_h\|_{L^2(\Gamma_-)^2}) \|V\|_{\mathcal{H}_{\text{qp}}^1(\Omega)}.
\end{aligned}$$

Then the proof is completed by using the above estimates in (42) and the inf-sup condition (14). \square

5. Implementation and Numerical Examples

This section presents the numerical implementation of the PML-AFEM algorithm by using the MATLAB toolbox, and validates the robustness of the proposed method through several numerical examples.

5.1. Adaptive algorithm

Based on Theorem 2, we can obviously see that the a posteriori error estimate contains two components, i.e., the FE discretization error ϵ_F and the PML approximation error ϵ_P , where

$$\epsilon_F = \left(\sum_{T \in \mathcal{M}_{h,+}} \eta_{T,+}^2 + \sum_{T \in \mathcal{M}_{h,-}} \eta_{T,-}^2 \right)^{1/2}, \quad (45)$$

$$\epsilon_P = F_1 \|\hat{p}_h^{\text{sc}}\|_{L^2(\Gamma_+)} + F_2 \|\hat{\mathbf{u}}_h\|_{L^2(\Gamma_-)^2}. \quad (46)$$

According to (46), we can select suitable PML parameters δ_j and σ_j satisfying $F_1 \Lambda^{1/2} \leq 10^{-8}$ and $F_2 \Lambda^{1/2} \leq 10^{-8}$ to significantly reduce the PML error. In our numerical experiments, we always take $m = 2$ and $\delta_1 = \delta_2 = \delta$. Algorithm 1 outlines the implementation steps of the adaptive P_1 -FEM algorithm.

Algorithm 1 Adaptive PML-FEM algorithm for the acoustic-elastic interaction in periodic structures

```

1: Set the incident angle  $\theta$  and the other parameters  $\rho, \rho_f, \lambda, \mu, \omega$ ;
2: Given the tolerance  $\text{tol} > 0$  and the threshold value  $\tau \in (0, 1)$ ;
3: Choose  $\delta$  and  $\sigma_j$  such that  $F_1 \Lambda^{1/2} \leq 10^{-8}$  and  $F_2 \Lambda^{1/2} \leq 10^{-8}$ ;
4: Construct an initial triangulation  $\mathcal{M}_h$  over  $D$ ;
5: Compute the numerical solution  $\hat{\mathbf{U}}_h$  of the problem (35) and calculate error estimators;
6: while  $\epsilon_F > \text{tol}$  do
7:   Modify the mesh  $\mathcal{M}_h$  based on the following strategy:
8:   if  $\eta_{T,+}/\eta_{T,-} > \tau \max_{T \in \mathcal{M}_h} \{\eta_{T,+}/\eta_{T,-}\}$  then
9:     Refine the element  $\hat{T} \in \mathcal{M}_h$ ;
10:    end if
11:    Solve the discrete problem (35) on the new mesh;
12:    Compute the corresponding error estimators;
13: end while

```

5.2. Numerical Examples

This subsection presents four numerical examples to demonstrate the robustness and effectiveness of the proposed adaptive strategy. In the first example, a scattering problem with an analytical solution is used to verify the accuracy of the method. The second and third examples are constructed such that the solutions have corner singularities. The last example focuses on a high-frequency case.

Example 1. In this example, the fluid-solid interface Γ is considered as a straight line with $x_2 = 0$. The parameters are chosen as $\omega = \pi$, $\rho = \rho_f = 1$, $\mu = \lambda = 1$ and $\theta = \pi/6$. Take $h_1 = 1$, $h_2 = -1$ and $\Lambda = 1$. According to [25], the analytical solutions can be written as

$$p^{\text{sc}}(\mathbf{x}) = q_1 e^{i(\alpha x_1 + \beta_0 x_2)}, \quad \mathbf{x} \in \Omega_+,$$

$$\mathbf{u}(\mathbf{x}) = q_2 \begin{bmatrix} \alpha \\ -\beta_0^{(1)} \end{bmatrix} e^{i(\alpha x_1 - \beta_0^{(1)} x_2)} + q_3 \begin{bmatrix} \beta_0^{(2)} \\ \alpha \end{bmatrix} e^{i(\alpha x_1 - \beta_0^{(2)} x_2)}, \quad \mathbf{x} \in \Omega_-,$$

where the coefficients $q_j \in \mathbb{C}$ ($j = 1, 2, 3$) can be obtained by solving the following linear equations

$$\begin{bmatrix} i\beta_0 & \omega^2 \rho_f \beta_0^{(1)} & -\omega^2 \rho_f \alpha \\ 0 & i2\mu\alpha\beta_0^{(1)} & i2\mu(\beta_0^{(2)})^2 - i\mu\kappa_2^2 \\ 1 & i2\mu(\beta_0^{(1)})^2 + i\lambda\kappa_1^2 & -i2\mu\alpha\beta_0^{(2)} \end{bmatrix} \begin{bmatrix} q_1 \\ q_2 \\ q_3 \end{bmatrix} = \begin{bmatrix} i\beta_0 \\ 0 \\ -1 \end{bmatrix}.$$

Fig. 3 presents the real parts of the exact and numerical solutions with $\kappa = 1$. Obviously, the numerical solutions agree well with the exact solutions, which demonstrates the effectiveness of our PML-based adaptive FEM algorithm. Let $e_h = \|\mathbf{U} - \hat{\mathbf{U}}_h\|_{\mathcal{H}_{\text{qp}}^1(\Omega)}$ be the a priori error. In Fig. 4, we show the $\log e_h - \log \text{DOF}$ and $\log \epsilon_F - \log \text{DOF}$ curves by utilizing the adaptive DtN-FEM method and the adaptive PML-FEM algorithm, respectively, where DOF denotes the number of nodes. Obviously, the convergence rates of the a priori and a posteriori errors are both $O(\text{DOF}^{-1/2})$. It can be seen from Fig. 4 that the error of the DtN-FEM method is smaller than the PML-FEM method at the same degrees of freedom. However, the PML method only needs to impose the Dirichlet boundary conditions, while the DtN method must handle the nonlocal boundary conditions. Thus, the PML method is much simpler than the DtN method in numerical implementation.

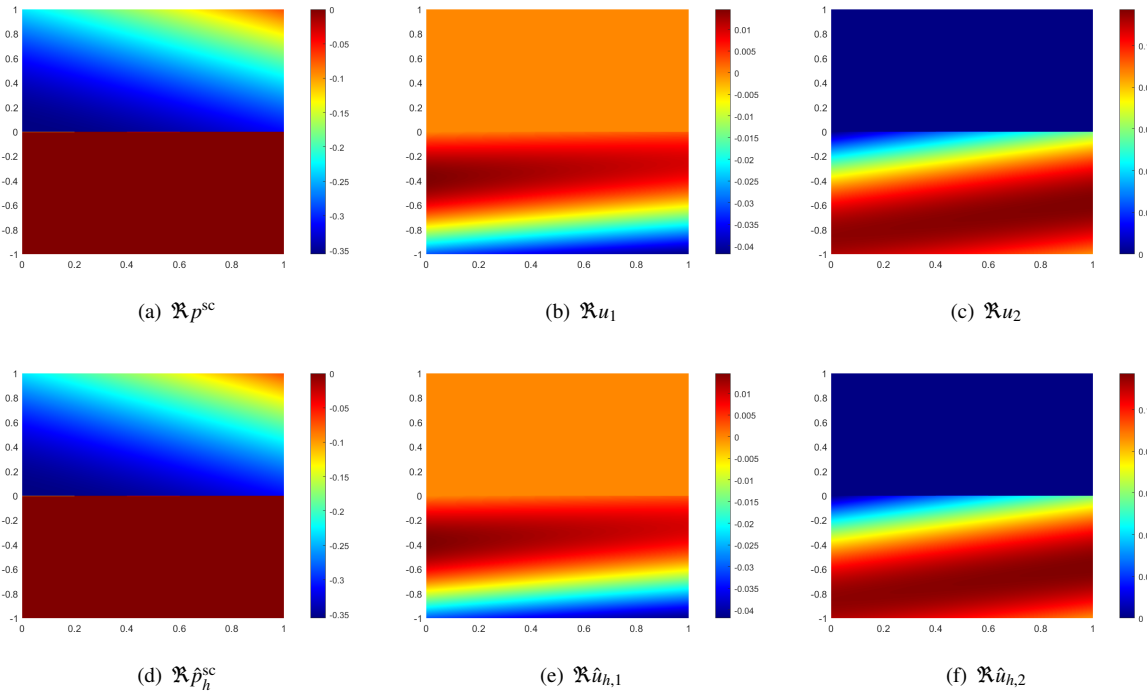


Figure 3: Example 1. Real parts of the exact solutions (a)-(c) and numerical solutions (d)-(f) with $\kappa = 1$.

Example 2. The grating surface is selected to have a sharp angle in this example. Let $\omega = 2\pi, \rho = \rho_f = \lambda = 1, \mu = 2, \theta = \pi/6$, and choose $h_1 = 1, h_2 = -1$. We plot the numerical solutions in Fig. 5 with $\kappa = 1$ and $\delta = 3$. Fig. 6 shows the initial mesh and the corresponding adaptive mesh around the corner points after five refinement iterations, where the adaptive mesh consists of 887 nodes and 1628 elements. It is clear to show that the algorithm does capture the solution feature and adaptively refines the mesh around the corners, where solution displays singularity. The a posteriori errors and the corresponding DOF for the uniform and adaptive refinements with $\kappa = 1$ and $\delta = 3$ are presented in Table 1. Obviously, the adaptive refinement can achieve the superior accuracy with fewer DOF compared with the uniform refinement, which illustrates the advantage of the adaptive strategy. Fig. 7 displays the log-log curves of the a posteriori error estimates against DOF with different wavenumbers κ and PML thicknesses δ , which show that the a posteriori errors are quasi-optimal.

Example 3. In this example, the grating surface is a trapezoidal structure. We choose $h_1 = 2, h_2 = -2$ and $\Lambda = 4$. The rest of the parameters are the same as those in Example 2. We set $\kappa = 1, \delta = 4$. The real parts of the numerical solutions as well as the corresponding adaptive mesh are displayed in Figs. 8 and 9, respectively. A numerical comparison between uniform and adaptive refinements is provided in Table 2. Once again, the algorithm

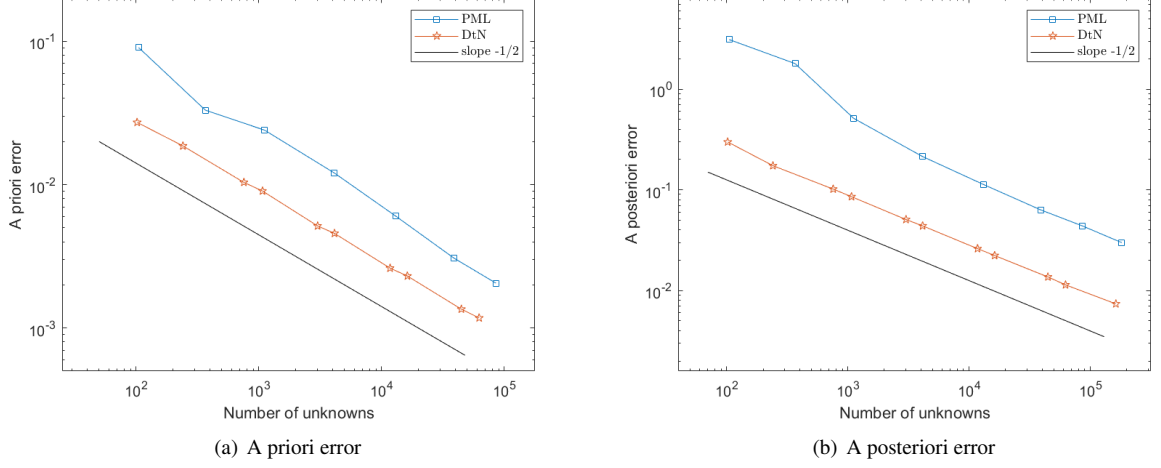


Figure 4: Example 1. Log-log curves of the error estimates versus DOF with $\delta = 1, 2, 3$: (a) A priori error; (b) A posteriori error.

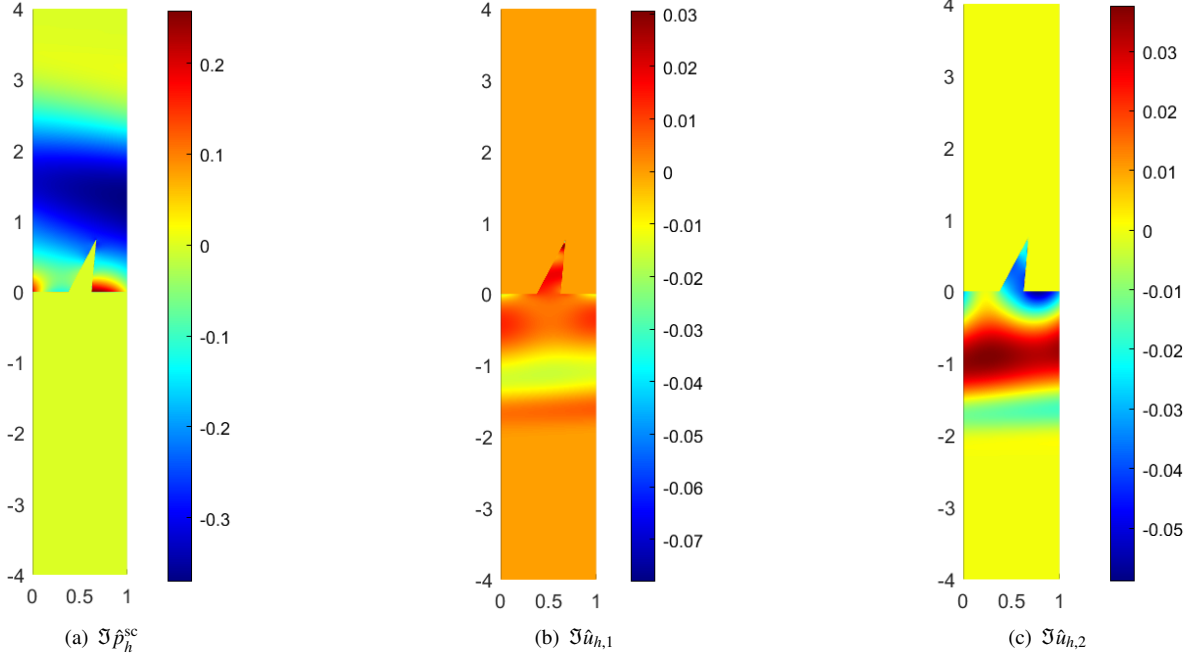
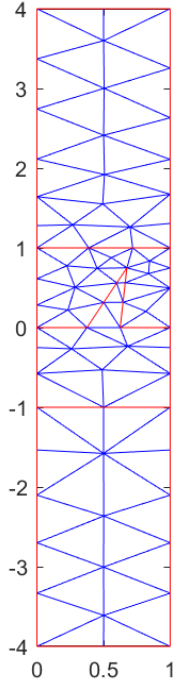


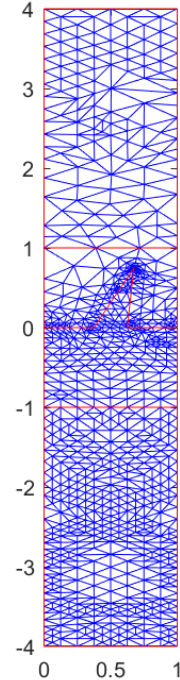
Figure 5: Example 2. Imaginary parts of the numerical solutions with $\kappa = 1$ and $\delta = 3$.

shows the ability to capture the singularity of the solution and perform local mesh refinements. In Fig. 10, the curves of $\log \epsilon_F - \log \text{DoF}$ are plotted for different κ and δ to demonstrate the quasi-optimal convergence rates of our proposed method.

Example 4. This example focuses on a high-frequency problem, where the grating surface has two sharp angles. We take the period $\Lambda = 2$. The remaining parameters are the same as those in Example 3. The real parts of numerical solutions with $\kappa = 20$ are presented in Fig. 11. Fig. 12 (a) demonstrates the quasi-optimality of the a posteriori error with different δ . Fig. 12 (b) displays the a posteriori errors against DOF with fixed $\delta = 4$ and different $\kappa = 10, 20, 30$,



(a) Initial mesh



(b) Adaptive mesh

Figure 6: Example 2. The finite element mesh: (a) Initial mesh with 70 nodes and 100 elements; (b) Adaptive mesh with 887 nodes and 1628 elements.

Table 1: Example 2. Comparison of the uniform and adaptive refinements in terms of DOF and the a posteriori error ϵ_F .

Uniform refinement		Adaptive refinement	
DOF	ϵ_F	DOF	ϵ_F
70	5.1176	70	5.1176
3353	0.5986	2842	0.4073
13105	0.2543	9786	0.2076
51809	0.1495	19700	0.1469
206017	0.1014	48264	0.0962

Table 2: Example 3. Comparison of the uniform and adaptive refinements in terms of DOF and the a posteriori error ϵ_F .

Uniform refinement		Adaptive refinement	
DOF	ϵ_F	DOF	ϵ_F
232	12.1684	232	12.1684
867	8.1307	610	5.5736
13161	2.4135	6455	2.3914
52177	1.2630	27369	1.2395
207777	0.6804	119932	0.5919

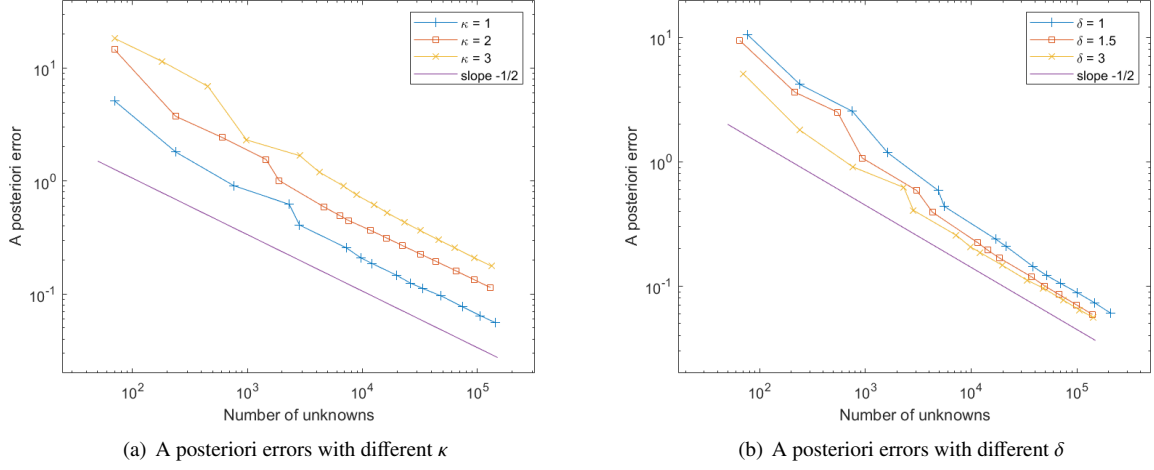


Figure 7: Example 2. Log-log curves of the a posteriori error estimates versus DOF: (a) For wavenumbers $\kappa = 1, 2, 3$; (b) For PML thicknesses $\delta = 1, 1.5, 3$.

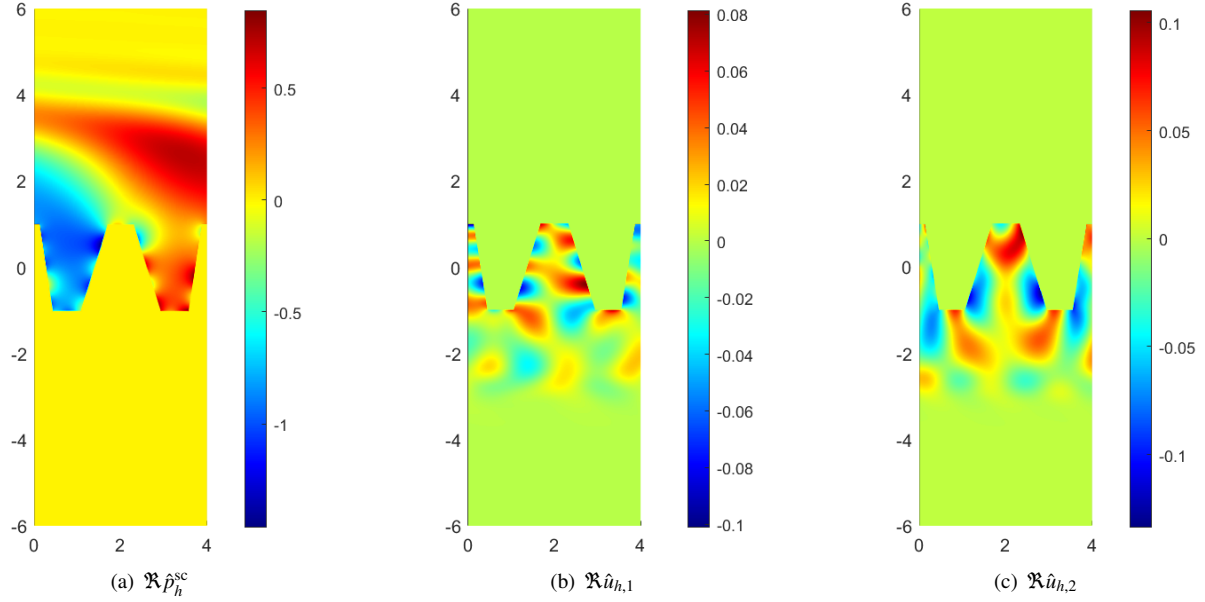


Figure 8: Example 3. Real parts of the numerical solutions with $\kappa = 1$ and $\delta = 4$.

which demonstrates that our adaptive PML-FEM algorithm is robust even for high-frequency problems. In addition, numerical results in Table 3 further confirm the superiority of the adaptive strategy.

6. Conclusion

We develop a PML-based adaptive FEM for solving the acoustic-elastic interaction problem in periodic structures. By introducing two PML-equivalent transparent boundary conditions, we prove the unique solvability of the truncated PML variational formulation and show that the PML truncation error decays exponentially as the PML parameters increase. We further give a residual-type a posteriori error estimate and develop an adaptive FEM algorithm to address

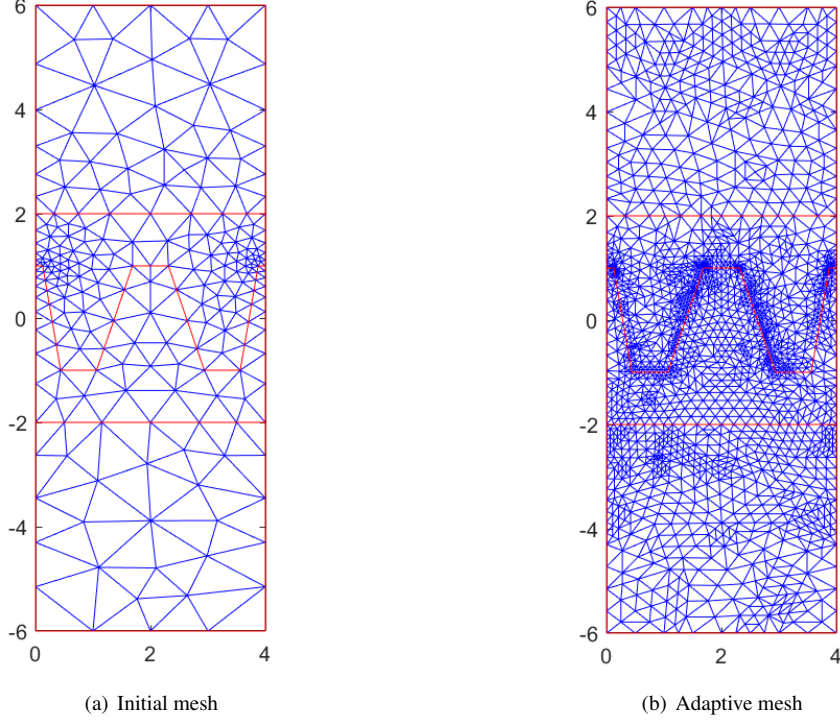


Figure 9: Example 3. The finite element mesh: (a) Initial mesh with 232 nodes and 404 elements; (b) Adaptive mesh with 1963 nodes and 3793 elements.

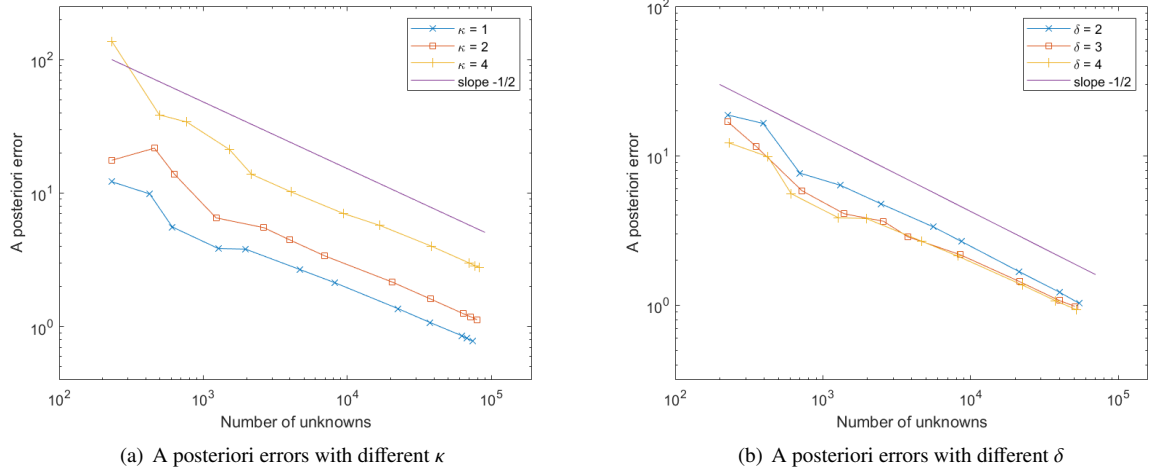


Figure 10: Example 3. Log-log curves of the a posteriori error estimates versus DOF: (a) For wavenumbers $\kappa = 1, 2, 4$; (b) For PML thicknesses $\delta = 2, 3, 4$.

singularities of the solution caused by the non-smooth fluid-solid interface. Numerical experiments are presented to validate the accuracy and robustness of the proposed method. Future work will extend the analysis of PML-AFEM to the thermoelastic scattering problem.

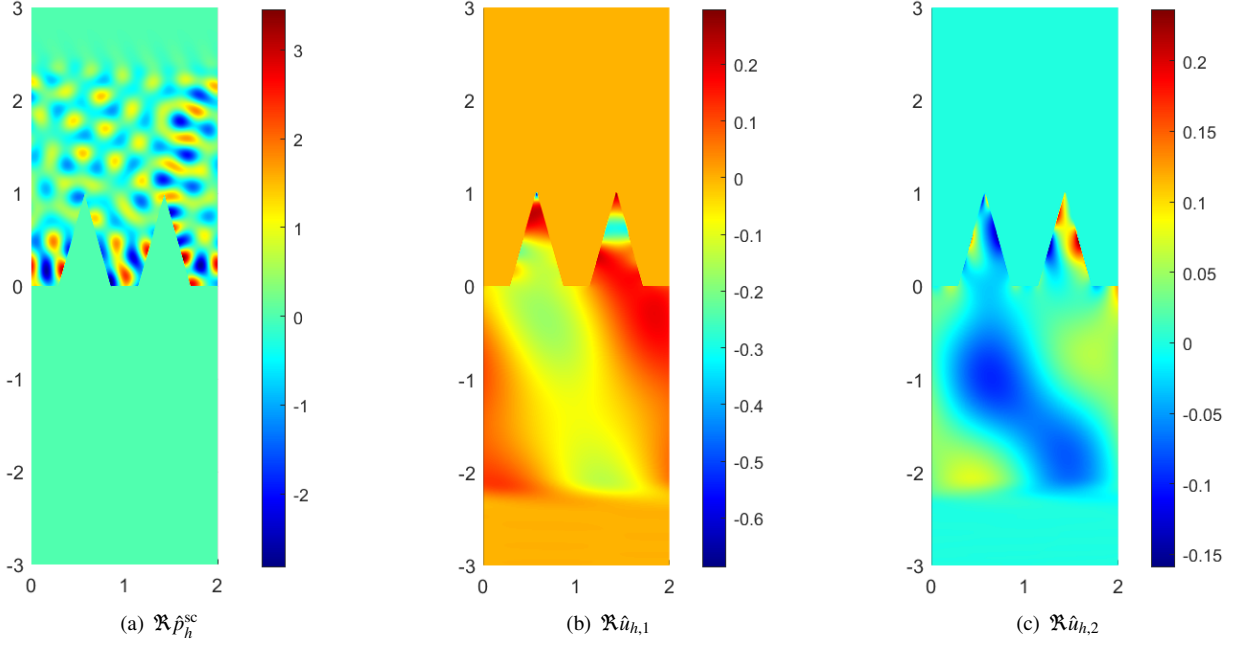


Figure 11: Example 4. Real parts of the numerical solutions with $\kappa = 20$ and $\delta = 1$.

Table 3: Example 4. Comparison of the uniform and adaptive refinements in terms of DOF and the a posteriori error ϵ_F .

Uniform mesh		Adaptive mesh	
DOF	ϵ_F	DOF	ϵ_F
95	112.6802	95	112.6802
4897	136.5494	2301	98.6562
19265	105.3166	4342	78.3530
76417	44.0865	21979	41.1862
304385	21.6798	149196	14.7741

Acknowledgment

This work of J.L. was partially supported by the National Natural Science Foundation of China (Grant No. 12271209).

Data availability

All data generated or analysed during this study are included in this article.

Declaration of competing interest

The authors declare that they have no known competing financial interests or personal relationships that could have appeared to influence the work reported in this paper.

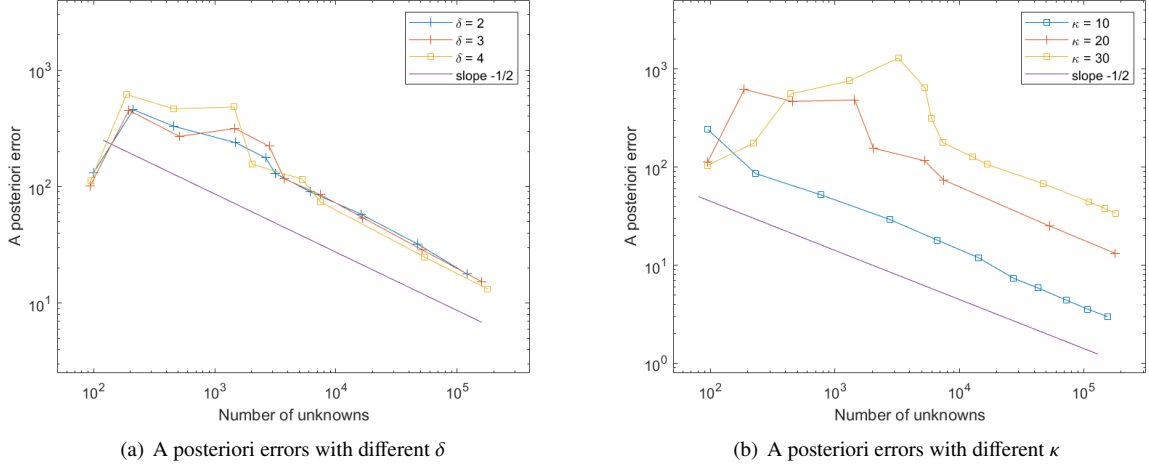


Figure 12: Example 4. Log-log curves of the a posteriori error estimates versus DOF: (a) For PML thicknesses $\delta = 2, 3, 4$; (b) For wavenumbers $\kappa = 10, 20, 30$.

References

- [1] M. Akköse, S. Adanur, A. Bayraktar, A.A. Dumanoglu, Elasto-plastic earthquake response of arch dams including fluid-structure interaction by the Lagrangian approach, *Appl. Math. Modelling* 32 (11) (2008) 2396–2412.
- [2] I. Babuška, W.C. Rheinboldt, Error estimates for adaptive finite element computations, *SIAM J. Numer. Anal.* 15 (4) (1978) 736–754.
- [3] G. Bao, L. Cowsar, W. Masters, Mathematical modeling in optical science, Society for Industrial and Applied Mathematics, 2001.
- [4] G. Bao, P. Li, Maxwell's equations in periodic structures, Springer, Singapore, 2022.
- [5] G. Bao, X. Jiang, P. Li, X. Yuan, An adaptive edge element method with perfectly matched absorbing layers for wave scattering by biperiodic structures, *Math. Comp.* 79 (269) (2010) 1–34.
- [6] G. Bao, W. Lu, T. Yin, L. Zhang, A highly accurate PML-BIE solver for the electromagnetic scattering problem in a multilayered medium, *SIAM J. Sci. Comput.* 46 (6) (2024) A3849–A3872.
- [7] G. Bao, H. Wu, Convergence analysis of the perfectly matched layer problems for time-harmonic Maxwell's equations, *SIAM J. Numer. Anal.* 43 (5) (2005) 2121–2143.
- [8] G. Bao, Y. Lin, Determination of random periodic structures in transverse magnetic polarization, *Commun. Math. Res.* 37 (3) (2021) 271–296.
- [9] J.-P. Berenger, A perfectly matched layer for the absorption of electromagnetic waves, *J. Comput. Phys.* 114 (2) (1994) 185–200.
- [10] J.H. Bramble, J.E. Pasciak, Analysis of a finite PML approximation for the three dimensional time-harmonic Maxwell and acoustic scattering problems, *Math. Comp.* 76 (258) (2007) 597–614.
- [11] J.H. Bramble, J.E. Pasciak, D. Trenev, Analysis of a finite PML approximation to the three dimensional elastic wave scattering problem, *Math. Comp.* 79 (272) (2010) 2079–2101.
- [12] J.M. Claeys, O. Leroy, A. Jungman, L. Adler, Diffraction of ultrasonic waves from periodically rough liquid-solid surface, *J. Appl. Phys.* 54 (10) (1983) 5657–5662.

- [13] J. Chen, Z. Chen, An adaptive perfectly matched layer technique for 3-D time-harmonic electromagnetic scattering problems, *Math. Comp.* 77 (262) (2008) 673–698.
- [14] Y. Chen, P. Li, X. Yuan, An adaptive finite element PML method for the open cavity scattering problems, *Commun. Comput. Phys.* 29 (5) (2021) 1505–1540.
- [15] Z. Chen, X. Liu, An adaptive perfectly matched layer technique for time-harmonic scattering problems, *SIAM J. Numer. Anal.* 43 (2) (2005) 645–671.
- [16] Z. Chen, H. Wu, An adaptive finite element method with perfectly matched absorbing layers for the wave scattering by periodic structures, *SIAM J. Numer. Anal.* 41 (3) (2003) 799–826.
- [17] Z. Chen, X. Xiang, X. Zhang, Convergence of the PML method for elastic wave scattering problems, *Math. Comp.* 85 (302) (2016) 2687–2714.
- [18] N.F. Declercq, J. Degrieck, R. Briers, O. Leroy, Diffraction of homogeneous and inhomogeneous plane waves on a doubly corrugated liquid/solid interface, *Ultrasonics* 43 (8) (2005) 605–618.
- [19] D.C. Dobson, Optimal design of periodic antireflective structures for the Helmholtz equation, *European J. Appl. Math.* 4 (4) (1993) 321–339.
- [20] B. Engquist, A. Majda, Absorbing boundary conditions for the numerical simulation of waves, *Math. Comp.* 31 (139) (1977) 629–651.
- [21] J. Gao, J. Lv, T. Niu, Uniqueness in inverse electromagnetic scattering by locally rough surfaces with phaseless near-field data, *Commun. Math. Res.* 41 (2) (2025) 189–208.
- [22] M.J. Grote, C. Kirsch, Dirichlet-to-Neumann boundary conditions for multiple scattering problems, *J. Comput. Phys.* 201 (2) (2004) 630–650.
- [23] T. Hohage, F. Schmidt, L. Zschiedrich, Solving time-harmonic scattering problems based on the pole condition. II. Convergence of the PML method, *SIAM J. Math. Anal.* 35 (3) (2003) 547–560.
- [24] G.C. Hsiao, W. Wendland, Boundary element methods: foundation and error analysis. In: Stein, E., de Borst, R., Hughes, T.J.R. (eds.) *Encyclopedia of Computational Mechanics*, vol. 1, pp. 339–373. Wiley, Amsterdam, 2004.
- [25] G. Hu, A. Rathsfeld, T. Yin, Finite element method to fluid-solid interaction problems with unbounded periodic interfaces, *Numer. Methods Partial Differential Equations* 32 (1) (2016) 5–35.
- [26] J. Huang, Z. Deng, L. Xu, A Bayesian level set method for an inverse medium scattering problem in acoustics, *Inverse Probl. Imag.* 15 (5) (2021) 1077–1097.
- [27] J. Huang, Z. Li, L. Xu, An extended sampling-Bayesian approach for inverse elastic scattering problems with limited aperture data, *Inverse Probl. Imag.* 22 (2025) 122–144.
- [28] X. Jiang, P. Li, An adaptive finite element PML method for the acoustic-elastic interaction in three dimensions, *Commun. Comput. Phys.* 22 (5) (2017) 1486–1507.
- [29] X. Jiang, P. Li, J. Lv, W. Zheng, An adaptive finite element method for the wave scattering with transparent boundary condition, *J. Sci. Comput.* 72 (3) (2017) 936–956.
- [30] X. Jiang, P. Li, J. Lv, W. Zheng, An adaptive finite element PML method for the elastic wave scattering problem in periodic structures, *ESAIM Math. Model. Numer. Anal.* 51 (5) (2017) 2017–2047.
- [31] X. Jiang, P. Li, J. Lv, W. Zheng, Convergence of the PML solution for elastic wave scattering by biperiodic structures, *Commun. Math. Sci.* 16 (4) (2018) 987–1016.
- [32] X. Jiang, P. Li, J. Lv, Z. Wang, H. Wu, W. Zheng, An adaptive edge finite element DtN method for Maxwell's equations in biperiodic structures, *IMA J. Numer. Anal.* 42 (3) (2022) 2794–2828.

[33] A. Kirsch, R. Zhang, The PML-method for a scattering problem for a local perturbation of an open periodic waveguide, *Numer. Math.* 157 (2) (2025) 717–748.

[34] P. Li, X. Yuan, Numerical solution to the PML problem of the biharmonic wave scattering in periodic structures, *IMA J. Numer. Anal.* draf025 (2025) Doi:10.1093/imanum/draf025.

[35] S. Li, L. Lin, J. Lv, A posteriori error estimate and adaptive algorithm of the finite element method for elastic scattering from anisotropic media with transparent boundary condition, *Internat. J. Numer. Methods Engrg.* 126 (22) (2025) Paper No. e70177.

[36] S. Li, J. Lv, T. Niu, A factorization method for inverse elastic scattering in cavity structure, *J. Sci. Comput.* 105 (1) (2025) Paper No. 6.

[37] S. Li, J. Lv, Y. Wang, Factorization method for inverse elastic obstacle scattering with Neumann boundary condition, *J. Sci. Comput.* 104 (2) (2025) Paper No. 45.

[38] Y. Li, H. Wu, Higher-order FEM and CIP-FEM for Helmholtz equation with high wave number and perfectly matched layer truncation, *J. Sci. Comput.* 104 (2) (2025) Paper No. 47.

[39] L. Lin, J. Lv, An adaptive finite element DtN method for the acoustic-elastic interaction problem in periodic structures, *Adv. Comput. Math.* 51 (4) (2025) Paper No. 41.

[40] L. Lin, J. Lv, J. Gao, An adaptive finite element DtN method for the acoustic transmission problem, *J. Comput. Appl. Math.* 471 (2026) Paper No. 116725.

[41] L. Lin, J. Lv, S. Li, An adaptive finite element DtN method for the acoustic-elastic interaction problem, *Adv. Comput. Math.* 50 (4) (2024) Paper No. 67.

[42] L. Lin, J. Lv, T. Niu, An adaptive DtN-FEM for the scattering problem from orthotropic media, *Appl. Numer. Math.* 209 (2024), 140–154.

[43] W. Lu, L. Xu, T. Yin, L. Zhang, A highly accurate perfectly-matched-layer boundary integral equation solver for acoustic layered-medium problems, *SIAM J. Sci. Comput.* 45 (4) (2023) B523–B543.

[44] W. Lu, W. Zheng, X. Zhu, Perfectly matched layer method for the wave scattering problem by a step-like surface, *SIAM J. Numer. Anal.* 63 (2) (2025) 744–771.

[45] T. Niu, J. Lv, J. Gao, Uniqueness and numerical method for phaseless inverse diffraction grating problem with known superposition of incident point sources, *Inverse Probl.* 40 (8) (2024) Paper No. 085006.

[46] L.R. Scott, S. Zhang, Finite element interpolation of nonsmooth functions satisfying boundary conditions, *Math. Comp.* 54 (190) (1990) 483–493.

[47] Y. Wang, L. Lin, J. Lv, Numerical method for the inverse scattering by random periodic structures, arXiv preprint, arXiv:2504.18356 2025.

[48] Y. Wang, J. Lv and S. Li, Numerical method for inverse scattering by random penetrable periodic structures, *Inverse Probl. Imag.* 19 (2025) 400–423.

[49] Z. Wang, G. Bao, J. Li, P. Li, H. Wu, An adaptive finite element method for the diffraction grating problem with transparent boundary condition, *SIAM J. Numer. Anal.* 53 (3) (2015) 1585–1607.

[50] L. Xu, T. Yin, Analysis of the Fourier series Dirichlet-to-Neumann boundary condition of the Helmholtz equation and its application to finite element methods, *Numer. Math.* 147 (4) (2021) 967–996.

[51] T. Yin, G.C. Hsiao, L. Xu, Boundary integral equation methods for the two-dimensional fluid-solid interaction problem, *SIAM J. Numer. Anal.* 55 (5) (2017) 2361–2393.

[52] W. Zhou, H. Wu, An adaptive finite element method for the diffraction grating problem with PML and few-mode DtN truncations, *J. Sci. Comput.* 76 (3) (2018) 1813–1838.